A Study of Lambda-Nucleon Scattering using the CLAS Detector

A thesis presented to

the faculty of

the College of Arts and Sciences of Ohio University

In partial fulfillment

of the requirements for the degree

Master of Science

Joseph A. Rowley

December 2018

This thesis titled

A Study of Lambda-Nucleon Scattering using the CLAS Detector

by

JOSEPH A. ROWLEY

has been approved for

the Department of Physics and Astronomy

and the College of Arts and Sciences by

Kenneth H. Hicks

Professor of Physics and Astronomy

Joseph Shields

Interim Dean, College of Arts and Sciences

Abstract

ROWLEY, JOSEPH A., M.S., December 2018, Physics

A Study of Lambda-Nucleon Scattering using the CLAS Detector (63 pp.)

Director of Thesis: Kenneth H. Hicks

Previous data for the elastic scattering of Lambda hyperons from the nucleon dates back to the bubble chamber era of the 1960s and 1970s. Data for Λ-N scattering is very limited in comparison with other elastic scattering processes, such as N-N, K-N or π-N. Using the high luminosity photon beam incident on a long (40 cm) liquid hydrogen target at Hall B of Jefferson Lab, the CLAS detector was used to identify a final state with a proton in coincidence with a scattered Lambda baryon. The Λ, before elastic scattering, were produced via the $\gamma p \rightarrow K^{+}\Lambda$ reaction, for which the cross section is well known. This allows us to determine the flux of Λ particles, with which we can then measure the Λ-p elastic scattering cross section in the momentum range between 0.6 and 1.6 GeV/c. Results from the analysis of this reaction are discussed as well as future work for the direction of this analysis.

Acknowledgments

I would like to thank Dr. Kenneth Hicks for his help and guidance through this project. I would also like to thank my committee members, Dr. Horacio Castillo and Dr. Daniel Phillips for taking time out of their schedules to play a role in this MS thesis. Finally, I would like to thank my friends and family for their never ending support.

Table of Contents

List of Tables

List of Figures

List of Symbols

Λ	Baryon consisting of an up, down and strange quark.
β	Velocity of a particle defined by the fraction of the speed of light, $\frac{v}{c}$.
N-N	Scattering or interaction between two nucleons (protons or neutrons).
Λ-N	Scattering or interaction between a Λ baryon and a nucleon.
K-N	Scattering or interaction between a K meson (kaon) and a nucleon.
π-N	Scattering or interaction between a π meson and a nucleon.
E_γ	Energy of a photon.
p_Λ	Momentum of a Lambda Baryon.

List of Acronyms

CEBAF Continuous Electron Beam Accelerator Facility. This is the accelerator at Jefferson Lab.

CLAS CEBAF Large Acceptance Spectrometer

TAG Electron Tagger

SC Start Counter

DC Drift Chamber

TOF Time of Flight Scintillator

CM Center of Mass reference frame

1 Introduction

There are four fundamental forces in the universe: strong, weak, electromagnetic and gravity. The goal of nuclear physics is to better understand the strong force. In order to examine the strong force we need to look at the particles that make up atoms themselves. Much like atoms are made up of nucleons in the nucleus being orbited by electrons, the nucleons are made up of particles called quarks. There are six types, or flavors, of quarks in total: up, down, strange, charm, bottom and top. In the case of the proton there are two up quarks and one down quark, and for the neutron there are two down quarks and one up quark. If we replace one of the quarks that make up a nucleon with a strange quark so that we have an up, down and strange quark, then we are left with a baryon known as Λ. The Λ is of interest because of its similarity to nucleons. In order to study such systems, scattering experiments are used.

Scattering experiments are useful to study the strong force, because they reveal how different particles interact with each other. One very useful measurement in nuclear and particle physics is a cross section. In classical mechanics, a cross section is dependent on the geometry and size of the two objects that are colliding. For example, two billiard balls only scatter if they physically touch each other. In particle physics scattering experiments, the particles interact with each other through the strong force. This allows for the cross section between two particles to be larger than the size of the particles. Therefore, our working definition of a cross section is a measure of the probability that two particles will interact.

Unlike nucleon-nucleon scattering, which has been extensively studied, there are very few data available for Λ-nucleon scattering. The current data that exists is shown in Figure 1.1.

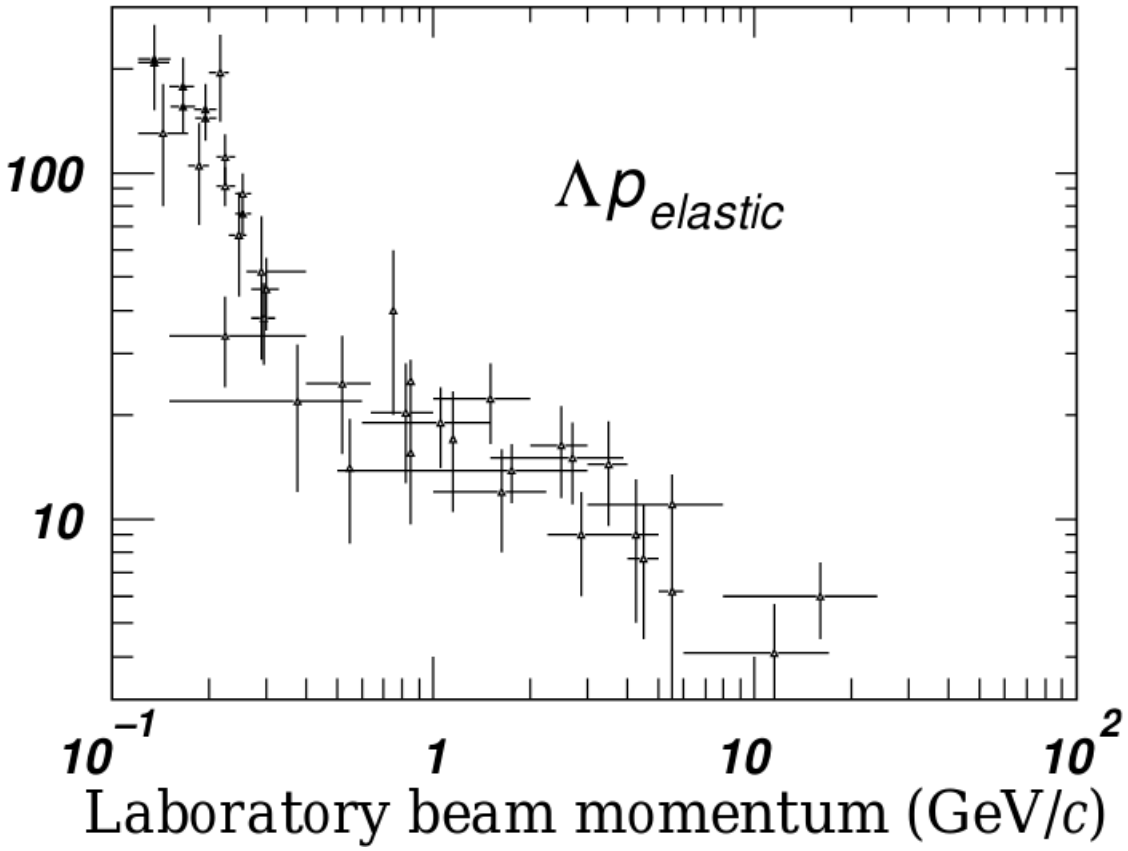

Figure 1.1: Existing Λ-N Cross Sections Data from [1]. Cross sections are measure in millibarn (10^{-27}cm).

It is clear that this data is limited. The reason for this is because all the current data we have comes from bubble chamber experiments. Bubble chambers were the primary way to detect particles in the 1960's and 1970's before modern accelerators and wire chambers allowed us to get more accurate measurements of particles at higher energies [4]. The reaction which will be looked at in this analysis is illustrated in Figure 1.2.

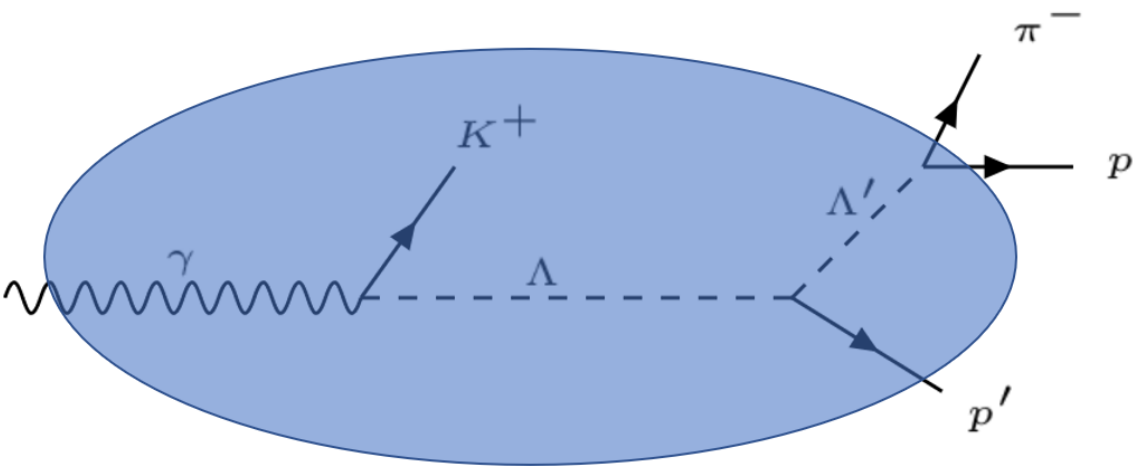

Figure 1.2: Pictorial representation of the reaction happening inside the target. A two part reaction occurs where a Λ beam is created and elastically scatters with a proton at rest in the target. What gets detected are two protons and a π^-, while the K^+ is identified through missing mass calculations.

A photon beam is sent into a liquid hydrogen target where it will collide with a proton at rest to create a K^+ and Λ baryon. The K^+ will not be detected but can be identified using missing mass calculations which will be discussed in Chapter 3. The Λ will then travel through the target until it either exits or elastically scatters with a second proton at rest. The recoiled proton can then be detected and the Λ will decay into a proton and pion, $\Lambda \rightarrow \pi^- p$, which will also be detected. So this analysis will discuss a two part reaction, however only the second part is of interest. The goal of this thesis is to provide better precision of the Λ-N cross section.

1.1 Theory

Scattering experiments involving nuclei go back to Ernest Rutherford who scattered alpha particles off of gold foil. This experiment showed that atoms were composed of a dense inner structure with positive charge, the nucleus, surrounded by negatively charged

electrons which orbited it. This led to what is now known as Bohr's model of the atom. The force responsible for this kind of scattering is the Coulomb force. As the positive alpha particles passed close by the positive charge of the gold nucleus, the repulsive force from the like charges caused the alpha particles to scatter. Modern day nuclear and particle experiments utilize similar methods to study the strong force. Particles are accelerated towards each other and scattered, so that information about the strong force can be gained. However, the nuclear force and the electromagnetic force are very different.

It is necessary to understand what happens during particle collisions. All particle interactions are mediated by exchanging other particles. For Coulomb scattering, as was done by Rutherford, the exchange particle was a photon. Figure 1.3 shows a Feynman diagram which illustrates this process but for the case of electron scattering. Two electrons move close to each other, and a photon is radiated by one and absorbed by the other. When the photon is first radiated, it carries some momentum away from the electron and when the second electron absorbs the photon, it also takes in the momentum. Without knowledge of this mechanism, it would appear that the electrons are hard shells which collide. This is a useful way to picture the interaction, but this particle exchange mechanism aids study of the fundamental forces.

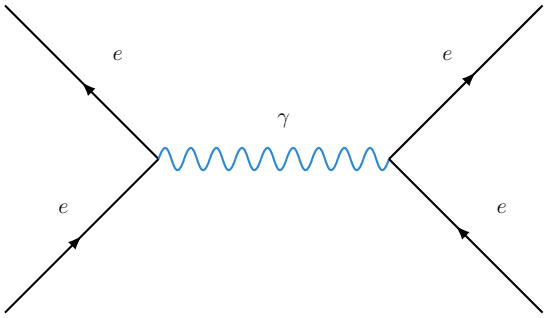

Figure 1.3: Feynman diagram representing a Coulomb scattering event where the exchange particle is a photon.

Transitioning from the electromagnetic force to the nuclear force, the most well studied scattering experiment is nucleon-nucleon(N-N) scattering. In 1934, Hideki Yukawa introduced the idea that N-N interactions were mediated by meson-exchange. Mesons are simply particles consisting of one quark and one anti-quark. Analogous to Figure 1.3 for the electromagnetic interaction, the Feynman diagram for the nuclear force is shown in Figure 1.4. The mediator in this case is a pion instead of a photon which, because the pion has mass unlike the photon, makes the nuclear force short range. The exchanged particle may be different, but the process can be thought of in the same way.

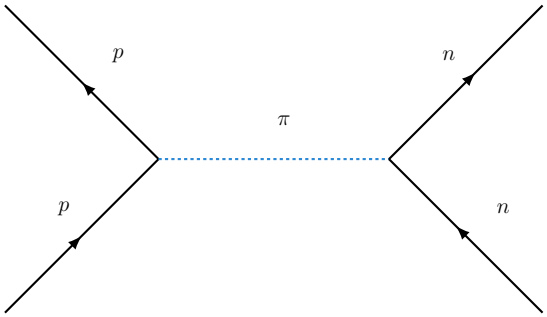

Figure 1.4: Feynman diagram representing a N-N scattering event where the exchange particle is a pion.

This meson-exchange nuclear potential is known as the Yukawa Potential [5]:

$$\phi(\mathbf{r}) = \frac{g}{4\pi r} e^{-\frac{mc}{\hbar} r} \tag{1.1}$$

where g is a scaling constant, c is the speed of light, $\hbar$ is the reduced Plank's constant, m is the mass of the mediating particle, and r is the distance from a point source. If we let $m = 0$ and $g = \frac{q}{\epsilon_0}$, then the Yukawa potential becomes the well known Coulomb potential:

$$\phi(\mathbf{r}) = \frac{q}{4\pi\epsilon_0} \frac{1}{r} \tag{1.2}$$

which describes the electrostatic potential of a charged point source in empty space. The connection between these potentials is that the Coulomb potential is simply a specific case of the general Yukawa potential. In the case of electrostatics, the particle that mediates the interaction between charged particles is the photon, which has no mass. For the nuclear force, $m \neq 0$ so the exponential term must stay. All this means is that for nuclear interactions, the particle exchanged when the nucleons interact has some mass. From this, Yukawa was able to predict the existence of the pion, before it was observed experimentally.

However, the reaction studied here is not N-N scattering, but rather Λ-N scattering. There are fundamental differences that make comparing to the N-N interaction wrong. As previously mentioned, the only difference between a nucleon and Λ is that the Λ replaces one of the up or down quarks with a strange quark. To explain this significance, a brief explanation of isospin is required. Protons and neutrons are almost the same particle. The proton has two up quarks, and one down quark while the neutron has two down quarks and one up quark. However, before scientists knew about quarks they noticed that protons and neutrons interacted the same way with the strong force, the only difference was their charge. So the idea of isospin was introduced which treats protons and neutrons as different states of the same particle, with only their charge to differentiate them. Since the strong force does not distinguish isospin, it remains a conserved quantity under strong interactions. This fits in well with the current quark model by assigning an isospin of $\frac{1}{2}$ to up and down quarks. All other quark flavors have isospin equal to zero. A third component, I_3, is $+\frac{1}{2}$ for up quarks, and $-\frac{1}{2}$ for down quarks. This means that protons and neutrons have an I_3 component of $+\frac{1}{2}$ and $-\frac{1}{2}$ respectively. Isospin conservation also limits strong force interactions, as the isospin before and after must not change. So for the case of N-N scattering, from Figure 1.4 a single pion as the exchange particle is allowed.

For Λ-N scattering, isospin prevents a single pion exchange because the pion has three charge states, giving it an isospin of 1. The Λ baryon has an isospin of zero, while the nucleon has an isospin of $\frac{1}{2}$. So a different mechanism is required to understand the Λ-N interaction. A possible exchange particle is the η. It is made up of a combination of up, down and strange quarks along with their anti-quarks (anti-up, anti-down and anti-strange). Therefore, since any up or down quark is always together with its anti-quark, the isospin of η is zero. Another candidate for the exchange particle are the ω mesons. These are mesons which are made up of up and anti-up quarks, or down and anti-down quarks. The ω meson has neutral charge only, which means its isospin is zero as well. Through scattering experiments, better understanding of these strong force interaction mechanisms can be gained.

2 Experimental Details

This analysis was done using the data from the g12 data set from the CEBAF Large Acceptance Spectrometer (CLAS) at Jefferson Lab in Newport News, Virginia [6]. The experiment consisted of a photon beam incident on a liquid hydrogen target. The target itself was a cylinder 40cm long by 4cm wide with the photon beam only incident on a 2cm diameter along the center of the target. An illustration of this is shown in Figure 2.1.

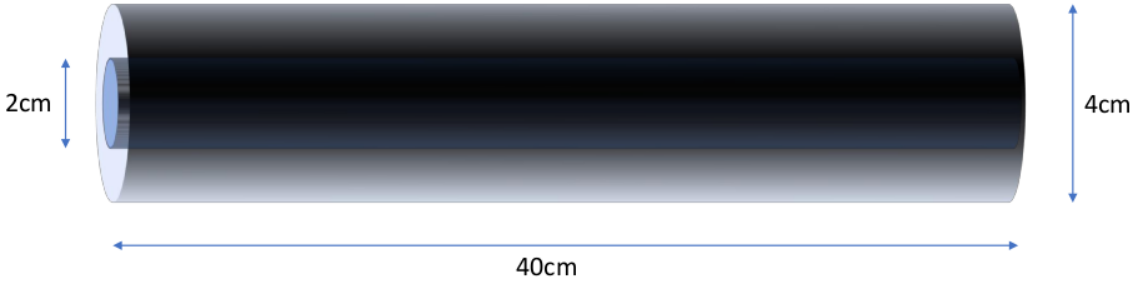

Figure 2.1: Dimensions of the liquid hydrogen target.

The photon beam was was created via Bremsstrahlung radiation after an electron beam was passed through a target of thin gold foil. The electrons then are exposed to a dipole magnet after passing through the gold target in order to bend them off the path, away from the hydrogen target. This allows only a photon beam to enter the target. Furthermore, there are electron taggers [7] (TAG), positioned to detect the electrons which were curved away from the path. These taggers allow us to measure both the energy of the electron, which in turn gives us the energy of the created photon, and the time the electron struck the tagger. This time can be used to determine when the photon was created and as will be explained later, allow us to determine which photon corresponds to which detected event. The incident electron beam had an energy of 5.7 GeV which created photon

energies in the range of 1.2 to 5.5 GeV. Figure 2.2 shows data for the energy distribution of the photons.

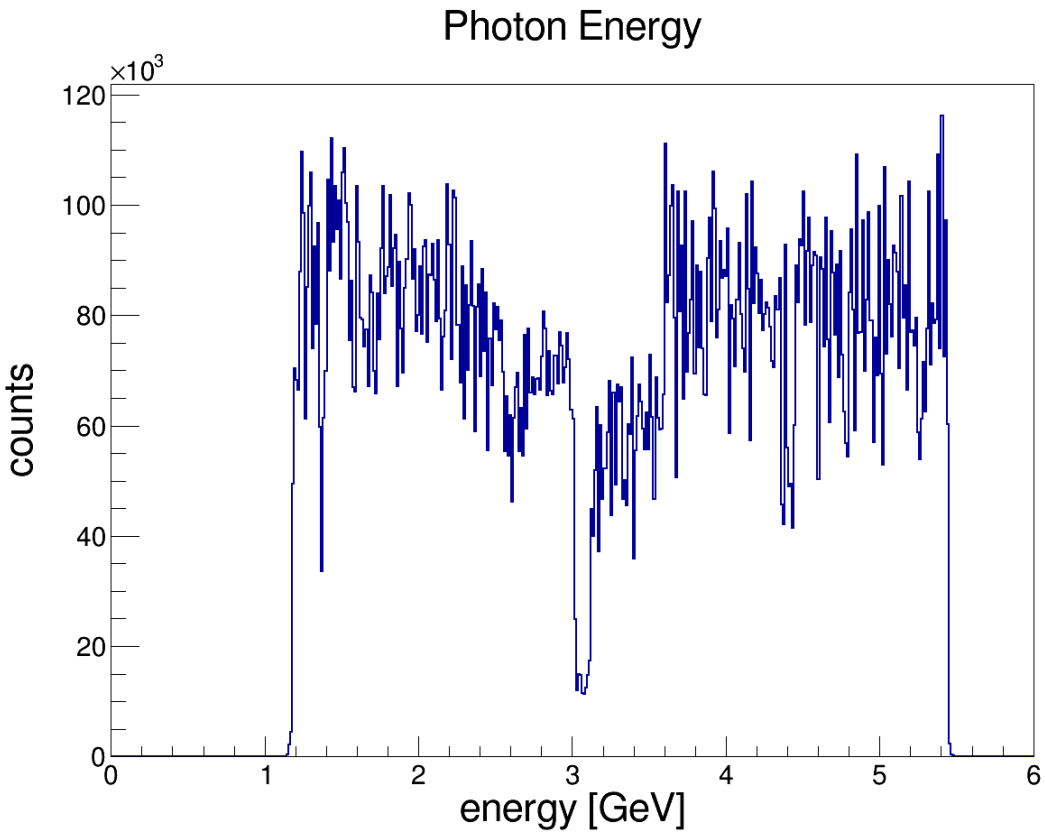

Figure 2.2: Photon energy spectrum for the g12 data set

The tagger allows the initial state of the reaction to be determined, since the photon energy is the only unknown value because the target is full of protons at rest. The final state detection requires more from the detector. As a note, it is important to keep in mind that there is an intermediate process occurring entirely in the detector. This reaction is of course, $\Lambda p \rightarrow \Lambda p$, which is what this experiment sets out to study. For now only detection of the final state particles will be discussed, and identifying these intermediate particles of

interest will be left for Chapter 3. Once the Λ and the proton elastically scatter, the Λ undergoes a decay, $\Lambda \rightarrow p\pi^-$. This is only one possible channel but the only one we look at in this analysis as the probability for this decay is 64%. The only other prominent channel is $\Lambda \rightarrow n\pi^0$ which has a decay probability of 36%. However, the products of this reaction channel would be difficult to detect in this experiment. Thus, all of the data from this reaction comes from the detection of the decayed proton and pion; along with the recoiled proton.

The detector itself is composed of six sectors as shown in Figure 2.3.

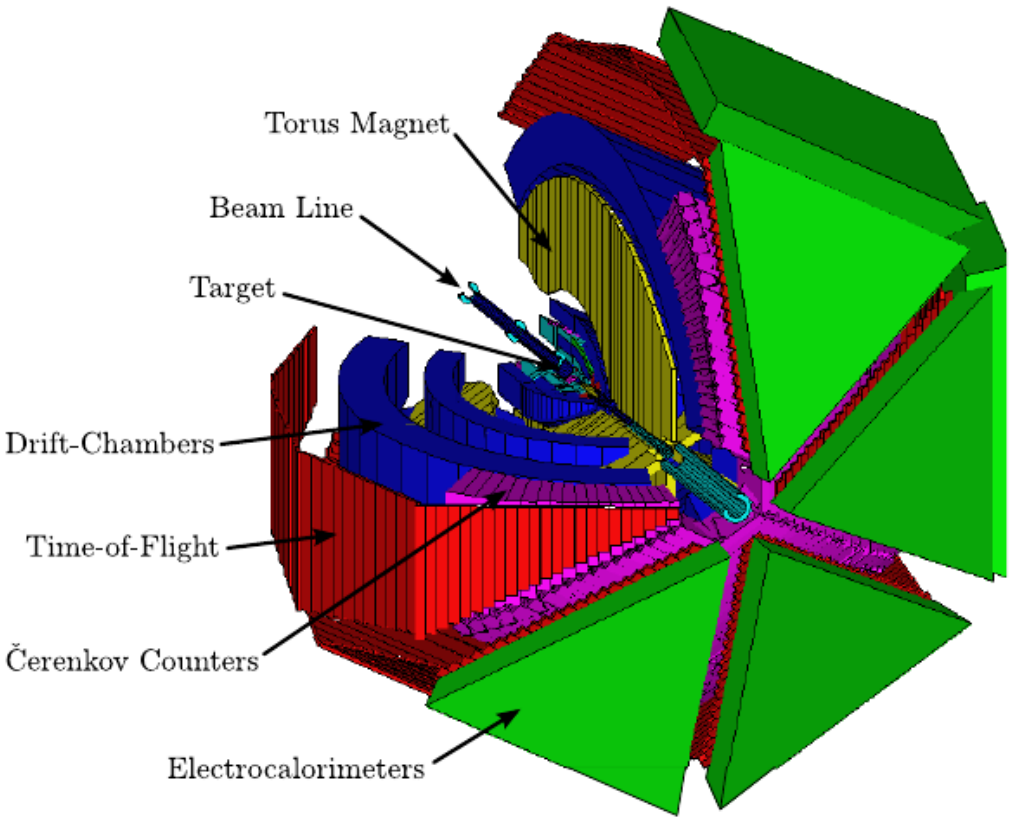

Figure 2.3: CLAS detector located in Hall B of Jefferson Lab with subsytems labeled. Figure reproduced from [2].

Each sector consists of a start counter (ST), drift chamber (DC), Cerenkov counter (CC), various time-of-flight scintillators (TOF), and an electromagnetic calorimeter (EC). For this analysis only the ST [8], DC [9], and TOF [10] were required. Once the final state particles exit the target they will interact first with the ST. It is made up of 24 scintillation paddles, four paddles for each sector, and surrounds the liquid hydrogen target. After the ST, the particles travel through three layers of drift chambers. The DC consists of multiple wires kept at a constant voltage. The chamber was full of gas which consisted of 90% argon and 10% carbon dioxide. This gas is easily ionized when charged particles pass through, which is the reason the $\Lambda \rightarrow n\pi^0$ is not studied in this analysis. These ionized particles then "drift" towards the charged wires and create a signal which can be measured. This can be done for every wire in the DC and the path of the particle can be tracked. There is an exterior toroidal magnetic field throughout the DC. The purpose of this is to bend the path of the charged particle as it travels through the chambers. Since the path through the DC can be observed, both the momentum and charge can be determined by measuring the deflection of angle of the particle. This method is further explained in Section 3.2. Once the particle exits the DC it is then detected by the TOF scintillator. The purpose of the TOF is to measure the time the particle interacted with the scintillator in order to identify it. Using timing coincidence between the TOF and the TAG allows identification of both the final state particle's and the incident photon, a process also discussed in Chapter 3. Since the momentum is determined by the DC, the energy measurement given by the TOF yields the four-momenta of the particle which is required to do any analysis.

3 Event Selection

Over the course of the experiment, many reactions are taking place and therefore many particles are coming out of the target and into the detector. We are only interested in events that have occurred from the reaction of interest. It is necessary to specify what is meant by "events", since it is potentially misleading. Each part of the detector can read off a signal, but none of these individual signals from every part of the detector is a triggered event. An event is when at least two tracks are in coincidence with the start counter. Specifically in our case, the tracks are that of a π^- and two protons. The tracks are identified by both the drift chamber and the time-of-flight detector. When the ST (start counter) and the TOF detector are hit within around 100s nanoseconds, then an event is recorded. Even with this condition, there are still other reactions we could observe. Furthermore, there is still background, primarily due to misidentification of particles, in the data that must be accounted for in the analysis.

3.1 Photon Selection

In order to do our analysis, we need to know the initial state of the reaction. For this, the photon which took part in our reaction must be identified. This is not always possible since the photons are created, via Bremsstrahlung radiation, in bunches timed 2-ns apart. The photon which collided with the proton to create a Λ has to be identified in the bunch in which it was created. In order to select the correct photon, the time of the initial reaction must be known. For a single particle track, the time of the reaction can be calculated from the TOF by:

$$t_{track} = t_{TOF} - \frac{d}{c\beta_c} \tag{3.1}$$

where t_{TOF} is when the TOF detector detected the particle, d is the distance from the beam vertex to the TOF detector, and β_c is the calculated velocity of the particle. The velocity is

calculated from the measured momentum by:

$$\beta_c = \sqrt{\frac{p^2}{m^2 + p^2}} \tag{3.2}$$

where m is the textbook mass of the identified particle. This same calculation can be done for all the tracks in the event. By averaging the time for each track, we get a time for the whole event, t_{event}. So far the only thing that was determined was the event time using only the detected, final state particles. To determine the photon that was involved in this event, we look at separate time measurement data from the electron Tagger.

Before the photon beam is created we first start with an electron beam. Electrons are what get accelerated in the tunnel, and after accelerating they collide with a thin gold foil to create a photon beam. These photons then go into the hydrogen target. They are created from Bremsstrahlung radiation and we can use the electron Tagger to measure both the momentum of the electron and the time it hit. From this, we also know the energy of the photon that was created and its time of creation. From this we can calculate the time the it took the photon to travel from its creation, to the event vertex:

$$t_{center} = t_{foil} + \frac{d'}{c}, \tag{3.3}$$

where t_{foil} is the time when the photon was at the foil, and d' is the distance from the gold foil to the center of the target. Ideally, $t_{center} = t_{event}$ because the photon should be at the event vertex at the same time the final state particles are. Using this, we can check each photon in the bunch to find which one was at the event vertex at the time of the detected particles. It is possible to still have more than one potential photon that fit this criteria. For this case, the energy of the photons must be looked at along with the energy of the final state particles. It is very unlikely to have more than one photon having the same time coincidence and an energy corresponding to $K^+\Lambda$ production.

3.2 Particle Identification

As many particles are being detected over the course of the experiment in the detector, it is necessary to identify the final state of the particles in the reaction we are examining, *i.e*. two protons and one π^-. From the SC, we know the time it took the particle to travel from the event vertex to the TOF detector. From this timing, and the known path the particle traveled in the DC, we can find the particles velocity from $v = d/t$. The DC also gives us the magnitude of the particle's momentum. From this we can calculate its mass:

$$m^2 = \frac{p^2(1-\beta_m^2)}{\beta_m^2} \tag{3.4}$$

in units where $c = 1$. This calculated mass can be compared to the masses of known particles. The particle whose mass best matches the mass calculated is then identified as the detected particle. However, to better improve measurements and to remove background events, analysis cuts are then done on the identified particles.

Once the particle has been initially identified, we can calculate the particles speed, β_c, from momentum measurements with the DC. Figure 3.1 shows the difference between the measured value of β, β_m, and the calculated value from the momentum and known mass of the three final state particles, $\Delta\beta = \beta_c - \beta_m$.

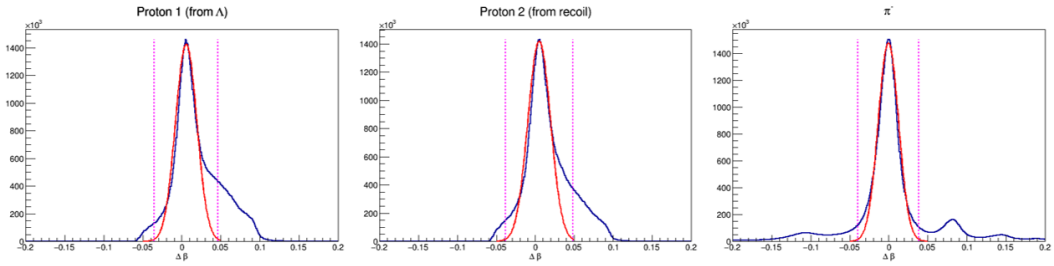

(a) Proton 1 (b) Proton 2 (c) π^-

Figure 3.1: Velocity measurements of each particle. Each particle was identified from its textbook mass and $\Delta\beta = \beta_c - \beta_m$ is shown on the horizontal axis.

Ideally, the calculated velocity and the measured velocity should be the same, $\Delta\beta = 0$. However, each particle shown in Figure 3.1 has a $\Delta\beta$ distribution. In the case of the π^- distribution, there are additional peaks not centered around $\Delta\beta = 0$. This is due to out-of-time photons, which are photons that came from a separate beam bunch than the photon that took part in the reaction. By fitting each distribution to a Gaussian function and cutting events that do not fall inside the function, each final state particle is better identified.

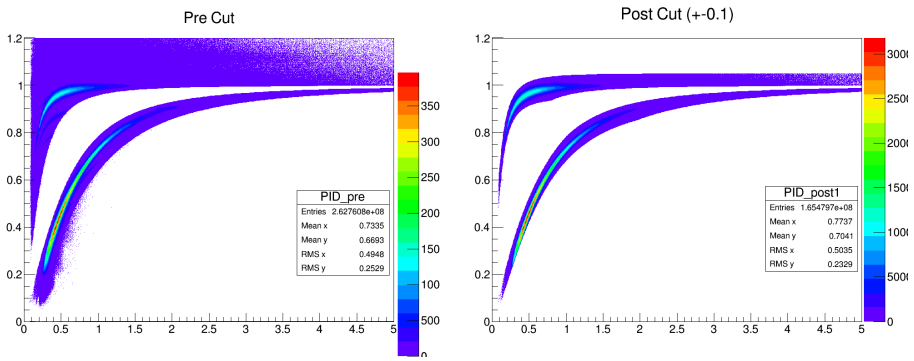

(a) Pre Cut (b) Post Cut

Figure 3.2: Particle identification plot before and after timing cuts were made. The plot is $\Delta\beta$ vs. p (units of GeV/c) and the bands represent identified particles. In this case, the higher band are pions and the lower band are protons.

Figure 3.2 shows the the momentum versus the measured value of β for the protons and the π^-. The top band is the detected π^- while the lower band are the protons. Most of the backgrounds which exist before the cuts are removed by this cut, but the main π^- and proton bands are left untouched.

Once the particles are correctly identified, then we know the momentum of each particle. From this and the textbook mass of each particle, we can calculate the energy:

$$E = \sqrt{m^2c^4 + |p|^2c^2} \tag{3.5}$$

The momentum and energy together gives us the four-momenta of the particle, which along with the vertex allows us to do the required analysis for this experiment.

3.3 Vertex Cut

From the drift chamber and the time of flight detector it is possible to identify a reactions starting vertex. It is expected that the reaction vertex lies within the target, however this is not always the case. Since we can identify the reaction vertex, the first cut

we make is to eliminate all events that appear to have been created outside the target. In Figure 3.3 we include only the region between the two apparent peaks. These peaks correspond to the walls of the target which contain the liquid hydrogen and are therefore not important to the reaction.

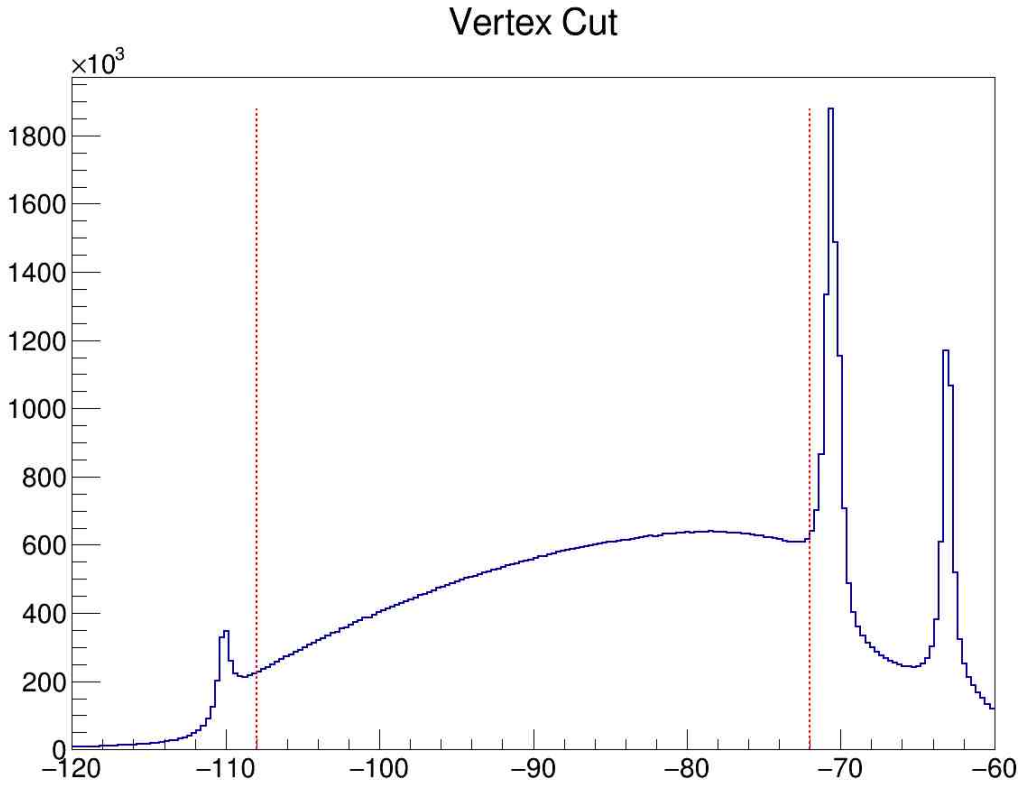

Figure 3.3: Vertex position (units of cm), projected onto the z-axis (parallel to the photon beam, for the secondary reaction).

The coordinate system here is defined so that z is along the photon beam, and therefore along the long side of the target. The negative values in the z-axis are due to the relative position of the target to the center of the detector. In the lab frame, the particles have

forward scattering, so the target was placed upstream of the detector's center in order to get a high sampling of events.

3.4 Fiducial Cuts

Not all areas of the detector are reliable. Data from the edges of the drift chambers are not as trust worthy as that from the center. Looking at the ϕ distribution (in the lab frame) of all π^- events in Figure 3.4 we can see regions which have a very low number of counts. This ϕ is the angle of the final state particle track in the xy-plane where the z-plane is the direction of the photon beam.

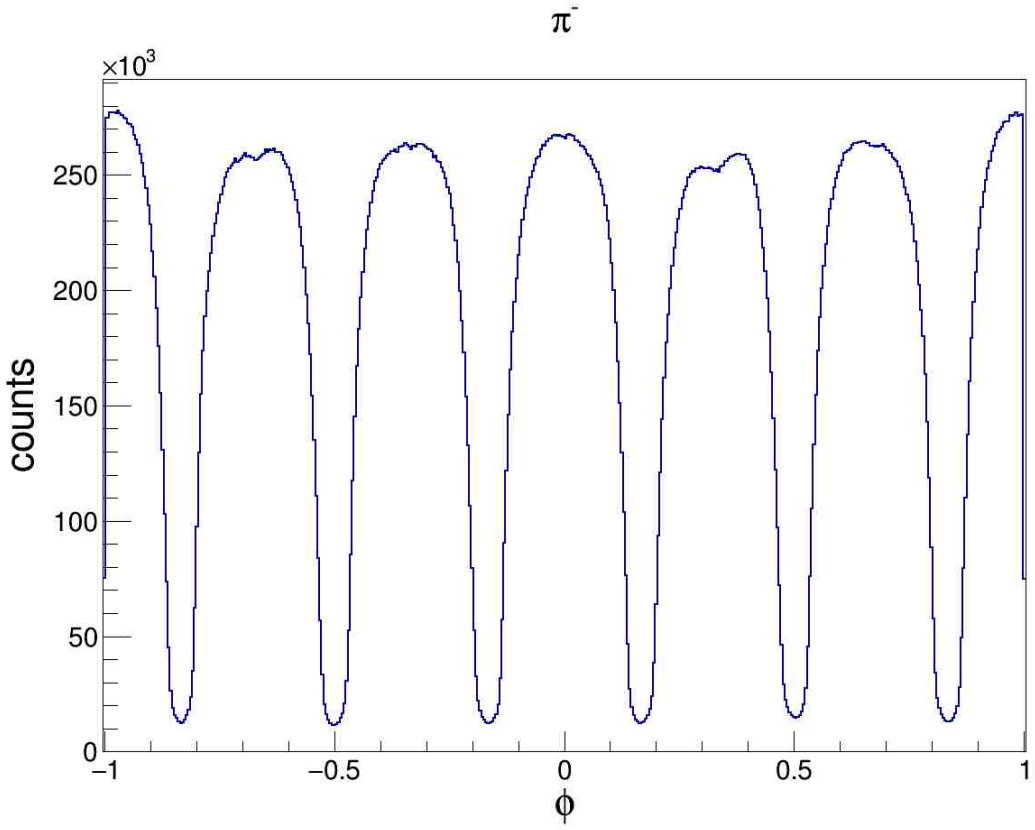

Figure 3.4: ϕ Distribution (units of radians/π of detected π^- particles.

In fact, these areas should have no data, as there is no detector. The question then becomes at what point do we include the data for analysis. The boundary which we cut at is determined for each sector separately.

The central region around each sector gets the largest number of events. The central region, which is defined $-10^o < \phi < 10^o$ have a relatively constant number of events across this area. At the edges of this region the counts start to drop off quickly, and nominal fiducial cuts remove those events at the edge of the sector once the count drops below 50% of the average number of events in the flat, central region. Figure 3.5 shows the events in the detector both before and after nominal fiducial cuts are applied. The spaces between each sector gets a dramatic decrease in the number of particles detected once fiducial cuts are made.

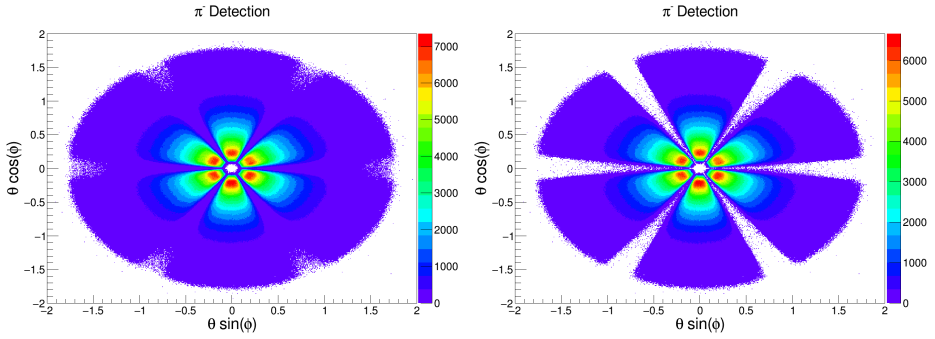

(a) Pre Fiducial Cuts (b) Post Fiducial Cuts

Figure 3.5: Angular distribution of the π^- before and after fiducial cuts from the reaction examined. Plotting is done to represent the geometry of the detector.

3.5 Λ' Identification

Since most of the particles detected in the good parts of the detector are not part of our reaction, there must be a process to cut out the excess data. The first cut we make is to eliminate all the events where we can not recreate a scattered Λ baryon. Even when we get events where we see a π^- and two protons as our final state particles, there is no guarantee that a Λ was created in the reaction. So cuts must be made around data which we know had a created Λ. Since the Λ decays into a π^- and a proton, we can recreate the scattered Λ by adding the four-momenta of each and checking the corresponding mass distribution to see if we can identify a distinguishing Λ peak. In Figure 3.6 there is a very notable peak at 1.115 GeV/c^2, which is the mass of a Λ.

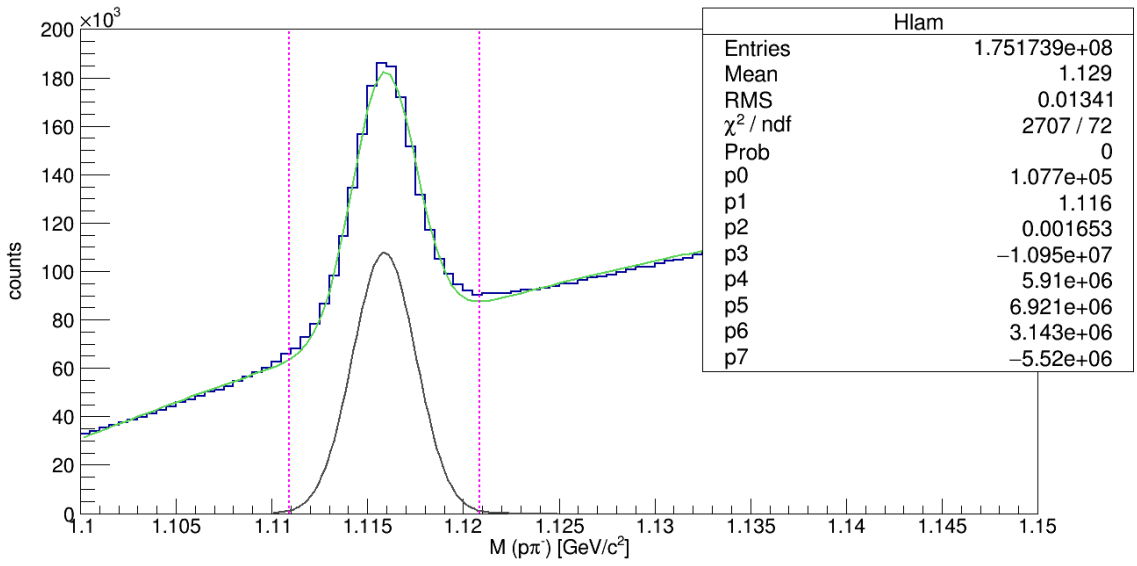

Figure 3.6: Combined mass of detected π^- and proton where a Gaussian was used to fit the peak around the mass of the Λ and cuts made at 3σ.

The peak centered at the Λ mass was fit to a Gaussian while the background was fit to a 2nd order polynomial. The background was then subtracted from the total shown by the Gaussian peak above. Cuts were made at 3σ, which includes data in which the invariant mass of the proton and π^- equals the Λ mass. There is also some ambiguity as to which proton the Λ decayed into along with the π^-. Figure 3.7, shows the mass distribution of the π^- with both protons. There is only a small region where the data overlaps. So, for almost all the data, we can be confident of which proton is associated with the Λ decay. For this reason, no additional cuts are made for the ambiguous protons.

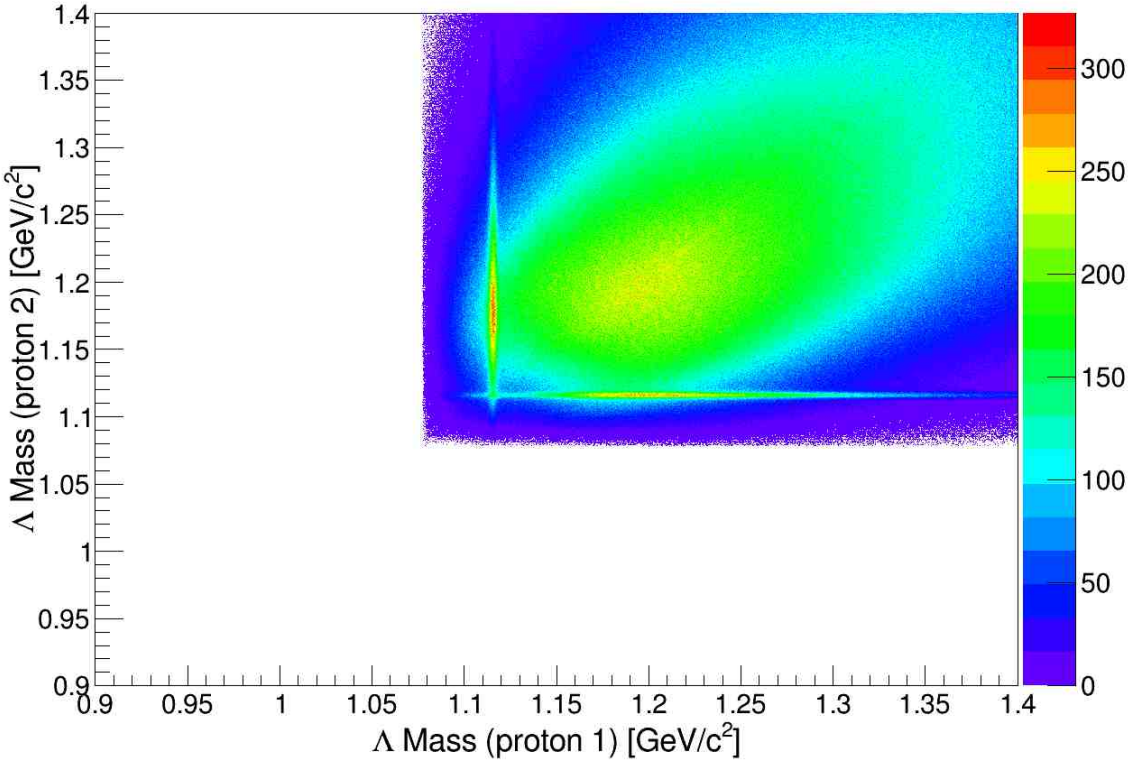

Figure 3.7: Comparing the invariant mass of the π^- and proton for each of the two detected protons to determine whether they can be distinguished.

3.6 Λ Identification

A second level of cuts can be made which identify the incident Λ, after the events which identified the scattered Λ'. The incident Λ is reconstructed using the four-momenta of the previously reconstructed scattered Λ, along with the scattered proton:

$$P_{missing} = P_{\pi^-} + P_{proton_1} + P_{proton_2} - P_{proton_{rest}} \tag{3.6}$$

Figure 3.8 shows the missing mass distribution which has a peak at the 1.115 GeV/c^2 (the mass of Λ). Once again, the peak was fit to a Gaussian while the background was fit it a 2nd order polynomial. By subtracting background we get a fit to the signal. Cuts are then made at 3σ.

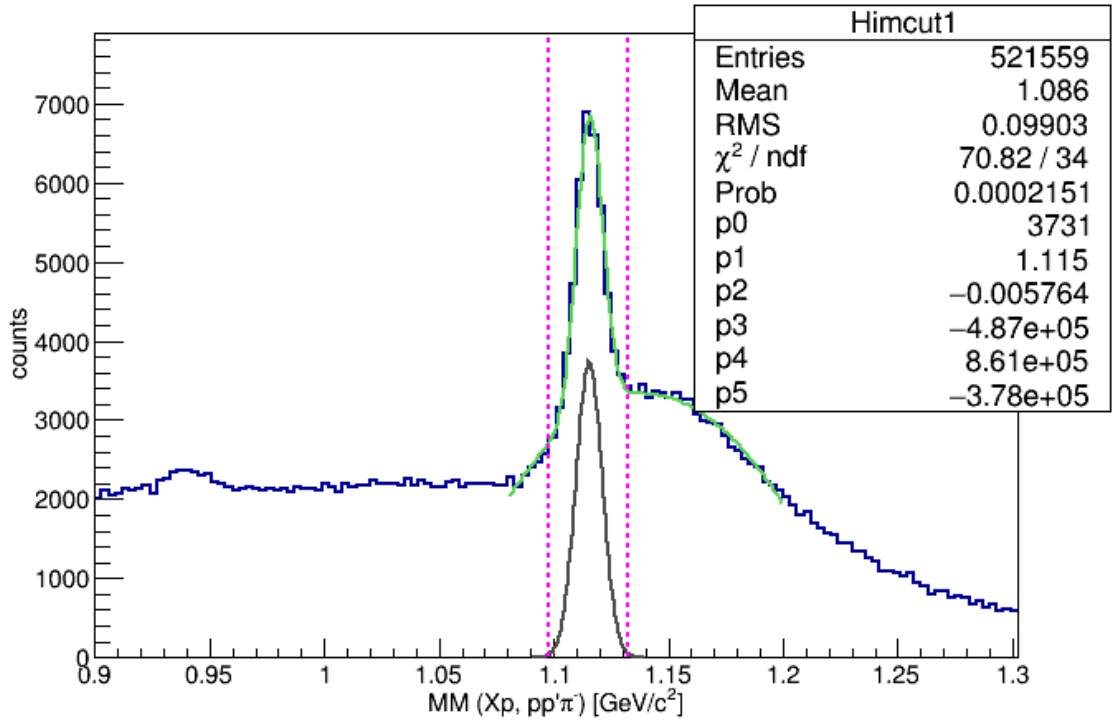

Figure 3.8: Missing Mass spectrum of secondary vertex where a Gaussian is fit to the peak around the mass of Λ and cuts made at 3σ.

At this point, only events which occur inside the target, and are detected by a reliable part of the detector will be analysed. Also, only events which check for an incident and scattered Λ will go through the analysis process.

3.7 Missing Mass of Primary Vertex

After all cuts are made we still need to check that an initial Λ was created. Since the first part of the reaction is $\gamma p \rightarrow \Lambda K^+$, we can use missing mass calculations to look for events which created a kaon. The missing mass four-momenta is calculated by:

$$MM = \gamma + p_{rest} + p_{rest} - (\pi^- + p_1 + p_2) \tag{3.7}$$

where all quantities are four-momenta, γ is the incident photon, p_{rest} are protons in the target, π^-, p_1 and p_2 are the final state particles that get detected. We then can calculate the invariant mass by taking the magnitude of the missing mass four vector. Figure 3.9 shows such a distribution.

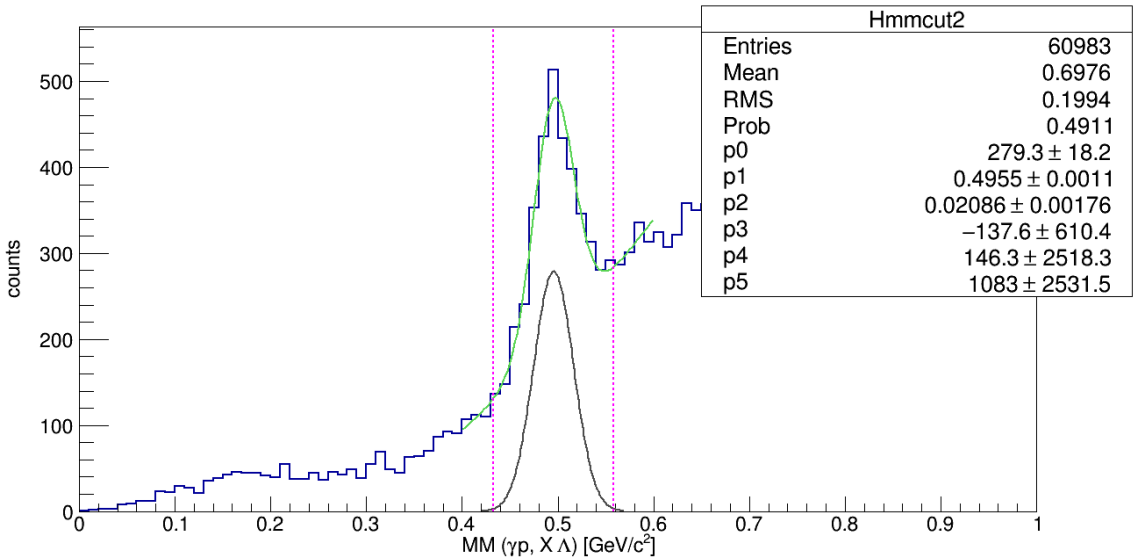

Figure 3.9: Missing mass distribution of the primary vertex with peak fit to a Gaussian and cuts made at 3σ.

The data shows a prominent peak at the mass of the kaon, $493.677\frac{MeV}{c^2}$. These are the events to do analysis on because after cuts are made, if we detect a kaon from missing mass, that means a Λ will have also been created. The peak was fitted with a Gaussian and the background was fitted with a second order polynomial. The background was then subtracted so that only the desired events remain. Further, we only look at events within 3σ of the Gaussian. These events will be used to find yield in section 4.1.

3.8 Sideband Subtraction

It is necessary to understand the background under the final missing mass distribution. To do this, we use the method of side-band subtraction. For the event selection, cuts were made around peaks in mass distributions which corresponded to particles of interest in the analysis. If we go back through the event selection process, and choose events on either side of the peak, but with the same width of the cut, we should only have background events in the final distribution. Figure 3.10 compares the final missing mass distribution $\gamma p \rightarrow X\Lambda$, for cuts which identify Λ and Λ' events, and those which do not. The cuts which do not include the identifications are called side-band cuts.

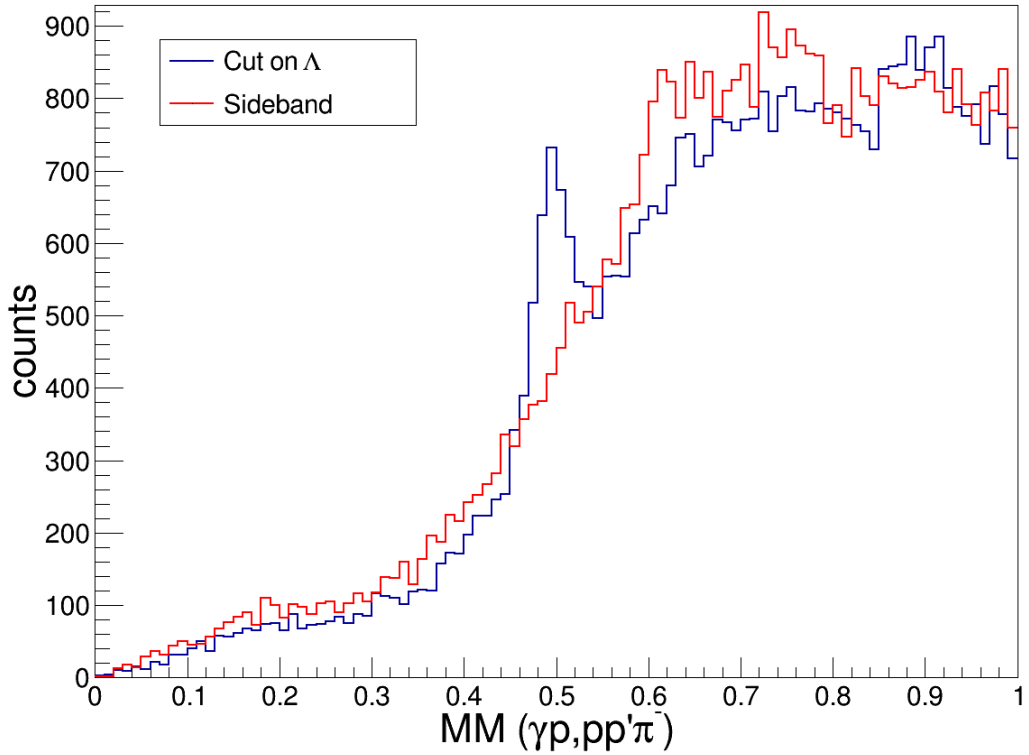

Figure 3.10: Comparing the missing mass (MM) distribution (units of GeV/c^2) with cuts made to include Λ events, and cuts made to exclude them

As we can see, the peak around the mass of the kaon is not present in the side band analysis, there is only background data. This verifies that our process is correct because if wrong cuts were being made, or the reaction was not properly identified, than there should not be a difference between the side-band missing mass spectrum, and the missing mass spectrum of interest. We can also compare the Λ momentum versus missing mass distribution as shown in Figure 3.11 for the data and for the side-band. The structure which corresponds to the invariant mass of the kaon only exists when we cut around the Λ events, while side-band spectrum has the same background distribution, but with a higher

density of events. The existence of the K^+ peak when only look at cuts which include the Λ and Λ' tell us that we are analyzing the correct reaction.

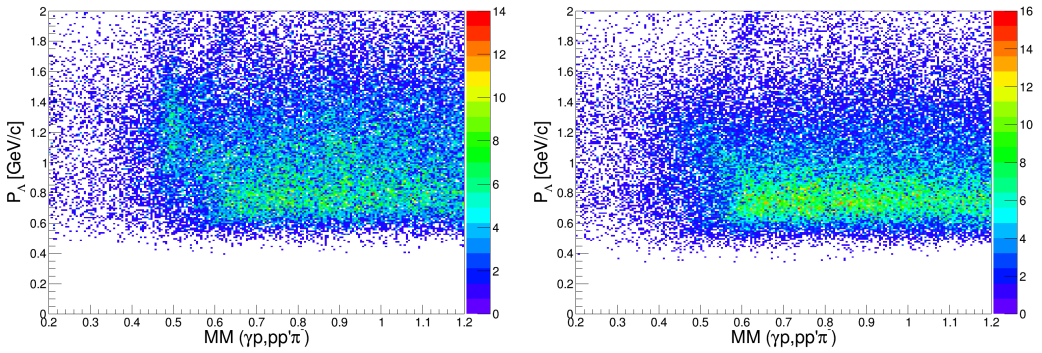

(a) Cut on Λ (b) Side-Band

Figure 3.11: Λ momentum (Lab) vs. Missing Mass spectrum for both cuts on Λ and Λ', and cuts on the side-band region.

It should be noted that there is some structure that becomes prevalent in the side band subtracted data. In the momentum range of 1.2 to 2.0 GeV/c there is a diagonal strip of data which most likely represents a final state that has not been taken into account. Regardless, it will not affect the rest of the analysis.

4 Analysis

As previously stated, the goal of this thesis is to improve the precision of the ΛN cross section. To this end, there are three quantities that need to be calculated in order to get a cross section: yield, luminosity and acceptance. From these, we can calculate the cross section from:

$$\frac{d\sigma}{dcos(\theta)} = \frac{Y}{A * \mathcal{L} * B.R. * dcos(\theta)} \tag{4.1}$$

where Y is the yield, A is the acceptance, $\mathcal{L}$ is the luminosity and $B.R.$ is branching ratio for the channel (0.64) [11].

4.1 Yield

Every part of analysis in Section 3 was done to obtain a yield. A yield is simply the number of Λp elastic scatters we see in the data. As previously discussed, many cuts need to be made to the data in order to identify events in which the reaction of interest occurred. Once these cuts are made, the yield can be extracted from the missing mass distribution in Figure 3.9. By counting the number of where we see a K^+, we also get the number of Λ. Further, since this cut was made after pre-scattered and post scattered Λ cuts were applied, these events are the ones to give us a yield. As discussed in section 3.7, the background was fit to a second order polynomial and subtracted from the peak, fit by a Gaussian, centered around $493.677\frac{MeV}{c^2}$ which represents K^+ events. This results in a Gaussian distribution of only the events and no background. The yield is simply the number of counts under the curve, which can be extracted by integrating the function. The integration limits are cut off at $\pm 3\sigma$. Integration of the Gaussian within the bounds yields a count of 1617 Λp scattering events coming from the $\gamma p \rightarrow K^+\Lambda$ reaction.

We must now bin the missing mass spectrum into incident Λ momentum, bins of p_Λ. The total yield for all the binned events should sum to approximately the yield of the global spectrum. Figure 4.1 shows the missing mass distribution of Figure 3.9, but with

each event binned in p_Λ. Each bin shows a distinctive peak at the mass of the K^+, which are the events we extract a yield from. Fitting is done the same way as for the global spectrum where the peak is fit to a Gaussian and the background is fit to a second order polynomial for each bin. The background is then subtracted to extract a Gaussian distribution of only the events, which is then integrated over, with limits at $\pm 3\sigma$.

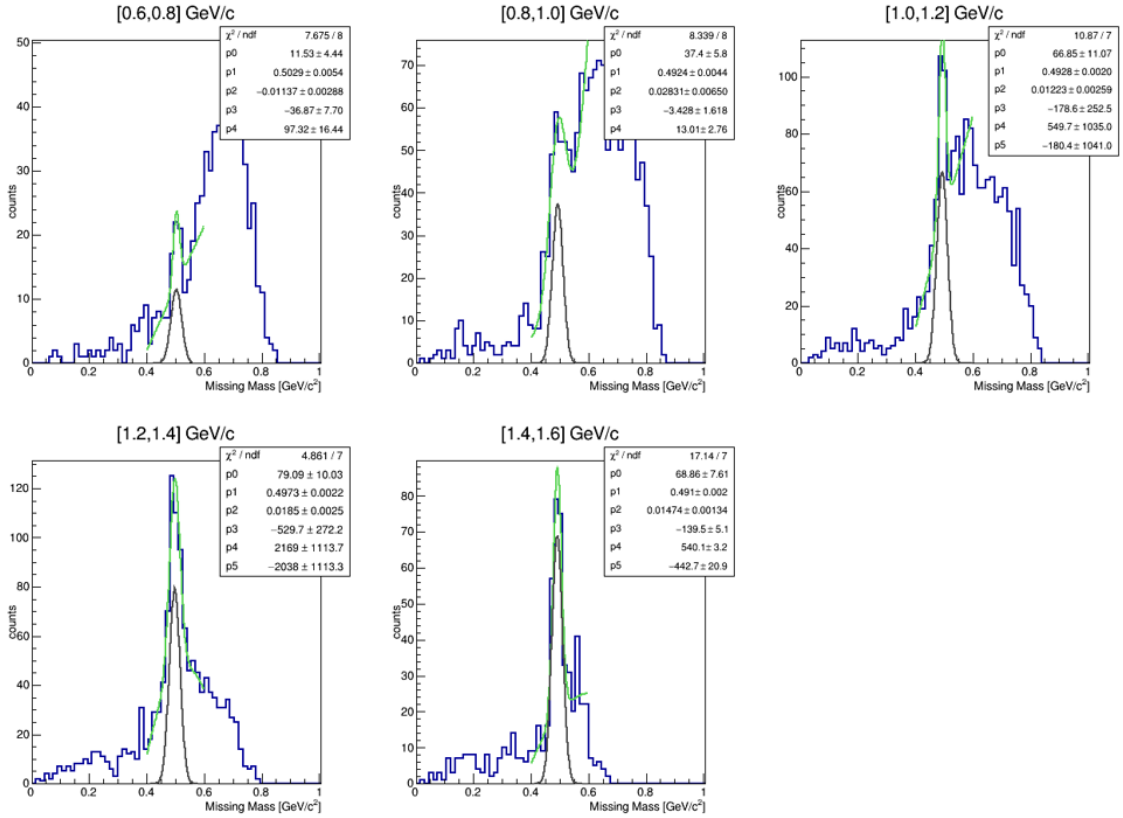

Figure 4.1: Missing Mass distribution binned in Λ momentum, with the bin limits shown in brackets above the plot.

4.2 Luminosity

Luminosity is a required part of the cross section calculation. It is a quantity that expresses the length the Λ particles are able to travel through the target. A single Λ can be created and travel the entire length of the target and exit without ever scattering with a proton. This is very unlikely however, since the Λ will most likely decay before traveling through the entire target. Some Λ may only travel a few millimeters, which is also unlikely. The collection of Λ particles will have an average path length which is determined by their momentum, and also by the number of particles in the beam. Note that the luminosity is indirectly related to the number of collisions which occur in the target. If all else remains constant and only the number of Λ particles in the beam, or the density of the target changed, then the number of collisions are also likely to change. In the case of the Λ beam in our experiment, the luminosity tells us the details of the beam. The luminosity can be calculated from:

$$\mathcal{L}(E_\Lambda) = \frac{N_A * \rho_T * l}{M} N_\Lambda(E_\Lambda) \tag{4.2}$$

where N_A is Avogadro's number, ρ_T is the mass density of the target, l is the average path length of the Λ beam, M is the molar mass of hydrogen and N_Λ is the number of Λ particles in the beam with incident energy E_Λ.

The luminosity calculation for this reaction is more involved than that of a one part reaction. Since the entire Λ beam exists inside the target, we never directly detect it, therefore it is difficult to normalize. It is important to distinguish this luminosity from that of the photon beam luminosity. The Λp cross section is dependent only on the Λ beam. To find this, we need to know how many Λ particles are being created in the target for each run, and the average path-length for the Λ beam. The difference between this case and that of a photon beam is that for the latter, we know both the flux of photons into the target, from the Tagger, and the average path-length. Unless the photons interact with the target,

almost all of them will pass through. The Λ beam on the other hand will, on average, not travel the length of the target and if it does not interact with a proton, it could decay inside the target. The mean proper lifetime of Λ is $c\tau$ = 7.89 cm, which is much less than the length of the target, 40 cm. So there are two things we must find in equation 4.2 in order to calculate the luminosity of the Λ beam: number of Λ, and the average path-length they travel in the target.

To calculate both of these variables, a simulation is done to model Λ particles in the target. Given a certain photon energy, E_γ, and Λ momentum range, p_Λ, simulated Λ are generated and the length each particle travelled is averaged. The decay probability equation [11]:

$$P(z) = e^{-\frac{M}{p}\frac{z-z_0}{c\tau}} \tag{4.3}$$

is used to calculate the distance each individual Λ traveled before it decayed. $P(z)$ is the probability that a Λ survives to the point z after being created at z_0. The momentum of the Λ is $p/c = M\beta\gamma$ in order to keep everything in the lab frame where the experiment takes place. From this decay equation, given a p, we can simulate any number of Λ and check how far each of them travel in the target. However, only Λ which move through the target go into the luminosity calculation. Figure 4.1 shows a simulation which generated 10,000 Λ particles and propagated them through the target. In this simulation all of the particles were given a momentum of 1.115 GeV/c, which is not the case in reality as all the Λ will have different momentum, but it is sufficient to make an observation.

If the Λ are all created at the front of the target and travel down the center, for this momentum they have an average path length of 7.5 cm. This is the same set up as a photon beam, except the Λ do not travel through the entire target. If the Λ are created at the center of the target with no angular distribution, they have only half the length of the target to travel. However, this is still quite far for most Λ and the average path length does not change much, only to 7.2 cm. Things really start to change when the Λ are created at

Table 4.1: Average path length ofparticles travelling through the target when given the same momentum under various starting conditions

Z Vertex (cm)	Cos(θ)	Avg. Pathlength (cm)
0.0	1.0	7.5
20	1.0	7.2
20	.707	2.4
Random	Random	2.2

an angle. The third row of Table 4.1 is when all of the particles are created at the center of the target, at a 45^o angle to the z-vertex. In this case the average path length changes drastically to 2.4. Further, in the fourth row the starting vertex and the angular distribution are randomized. The average path length does not change much but is still reduced to 2.2 cm. This emphasizes the importance of the angular distribution as it will have a great impact on the luminosity. The reason for this significant difference in path length is straight forward. Since the width of the target is relatively small compared to its length, only 4 cm, the Λ particles have less distance to travel before leaving the target. For example, a particle which starts in the center of the target traveling down the z-axis has 20 cm to travel before it leaves the target and stops contributing to the luminosity. However, if that same particle traveled perpendicular to the direction of the photon beam, it only has 2 cm to go before it leaves the target. So, there needs to be a way to simulate the angular distribution of the Λ in the target.

The method for finding the angular distribution and number of Λ both require knowledge of the $K^+\Lambda$ cross section. The cross section can be calculated by:

$$\sigma = \frac{N_\Lambda}{\mathcal{L}_\gamma} \tag{4.4}$$

where N_Λ is the number of Λ and $\mathcal{L}_\gamma$ is the luminosity of the photon beam. The energy dependent $K^+\Lambda$ cross section has already been studied and we use results from [3] shown in Figure 4.2.

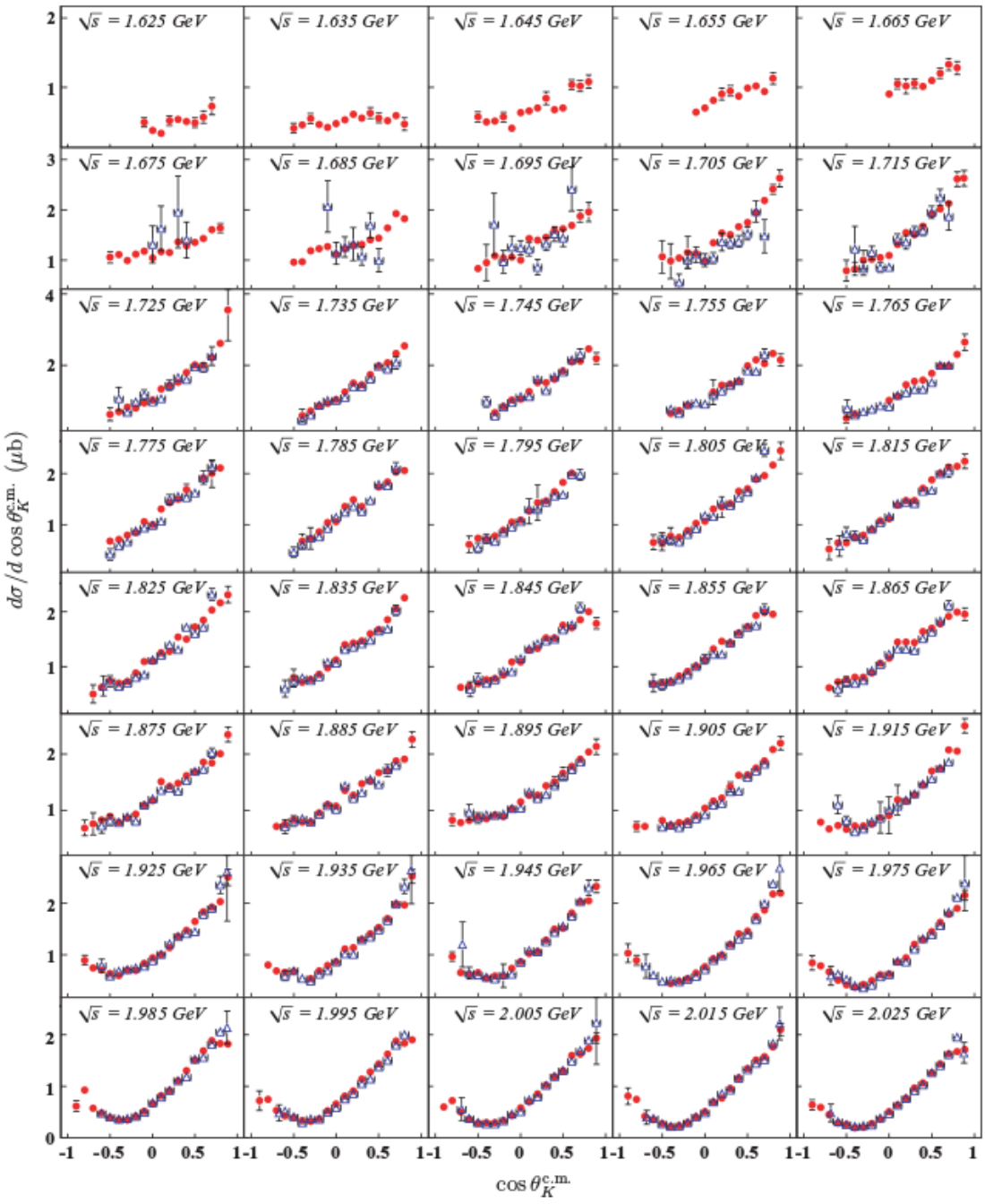

Figure 4.2: Published cross section for the $\gamma p \rightarrow K^{+}\Lambda$ reaction [3]. License permissions [1].

This data makes it possible to simulate a Λ beam with an angular distribution based on physical results.

The simulation randomly generates Λ particles uniformly throughout the target with a physical angular dependence. The reason we assume a random uniform distribution throughout the target is because the attenuation length of a photon in a hydrogen target is relatively large compared to the length of the target. An example of a mean free path for an average photon through the target can be calculated as follows:

$$m.f.p. = \frac{1}{\sigma\rho_N} = \frac{1\frac{g}{mol}}{30\times10^{-27}cm^2\times.071\frac{g}{cm^3}\times6\times10^{23}\frac{1}{mol}} = 782cm \tag{4.5}$$

where σ is the $\gamma p \rightarrow K^+\Lambda$ cross section and ρ_N is the number density of the atoms in the target. This tells us the average length a photon will travel in a sea of protons with the density of our target is 782 cm; which is much greater than the 40 cm target itself. This means that every point in the target is equally likely to create a Λ particle, which is why the simulation creates a Λ at a random position along along the length of the target. Also, since the photons enter the beam within a 1 cm radius from the center of the z-axis of the target, that position is randomized as well. The Λ for each run are created with the same photon energy which corresponds to the binning scheme of Figure 4.2. Ref. [3] defines the energy bins by $\sqrt{s}$, which is:

$$\sqrt{s} = \sqrt{m_p^2 + 2E_\gamma m_p} \tag{4.6}$$

where m_p is the mass of a proton and E_γ is the photon energy. So for each cross section, the binning can be done in E_γ. For each energy bin, ten thousand Λ are generated, all using the same initial photon energy. However, it is not enough to know E_γ and the angular distribution. There are physical limits on scattering angle of the Λ that is still not accounted for. The cross sections from Figure 4.2 are for the K^+ particle in the center of mass frame. The mass of Λ is greater than that of K^+ and therefore, even if the K^+ scatters maximally at 90^o, there is a limit to the maximum angle of the Λ scattering. There is also

a minimal angle Λ can scatter. So, when we simulate a Λ angular dependence, the range of the scattering angle must be limited. Limits are put in place by the momentum of the scattered Λ particle. Binning in Λ momentum, p_Λ, fixes the angular range of scattered Λ relative to photon beam axis, θ_Λ. The parameter p_Λ is binned in to relate to our binning scheme for the data. The maximum and minimum θ_Λ can be calculated, given E_γ and a range of p_Λ, by:

$$cos(\theta)_{K^+} = \frac{t + 2E_\gamma E_{K^+} - m_{K^+}^2}{2E_\gamma p_{K^+}} \tag{4.7}$$

where E_γ and E_{K^+} are the energies of the photon and kaon respectively, m_{K^+} is the mass of the kaon, and t is one of the Mandelstam variables. The Mandelstam variables are Lorenz-invariants and the t variable in equation 4.7 is defined as [12],

$$t = (\boldsymbol{p_\gamma} - \boldsymbol{p_{K^+}})^2 = (\boldsymbol{p_\Lambda} - \boldsymbol{p_p})^2 \tag{4.8}$$

where $\boldsymbol{p_\gamma}$, $\boldsymbol{p_{K^+}}$, $\boldsymbol{p_\Lambda}$, $\boldsymbol{p_p}$ are the four-momenta of the photon, K^+, Λ and proton respectively. The simulation takes E_γ as a parameter, as well as the momentum range of Λ. This gives us the energy of the Λ particle from $E_\Lambda = \sqrt{p_\Lambda^2 + m_\Lambda^2}$. The energy of the kaon can be found using conversation of energy:

$$E_{K^+} = E_\gamma + m_p - E_\Lambda \tag{4.9}$$

The maximum p_Λ in our binning range will yield one limit for $cos(\theta)_\Lambda$, while the minimum p_Λ will yield another. With this, we are able to simulate a Λ beam and calculate a luminosity. This calculation is further explained in the Appendix. The simulation proceeds as follows:

1. A E_γ is chosen based on the data from our experiment. This energy is then used to identify the desired bin from Figure 4.2.

2. For a range of p_Λ, limits of $cos(\theta)$ are identified using equation 4.7.

3. A p_Λ in the range of the maximum and minimum momentum defined by the bin is randomly generated.

4. Several Λ particles are randomly generated, weighted by the cross section distribution found in Figure 4.2 for the given E_γ and $cos(\theta)$ range. The cross sections which correspond to the $cos(\theta)_\Lambda$ values randomly generated are averaged. Using equation 4.4, where σ is now the average cross section over all events, N_Λ can be calculated.

5. The generated Λ are allowed to move and either decay or leave the target. This is done by generating a probability distribution based on equation 4.3 and allowing the particle to take a "step" of 1mm through the target. The particle is checked each step to see if it has decayed or left the target. If it is still in the target, another step is taken and the program continues.

6. The path length of each particle is averaged over ten thousand events, giving us the average path length, l, which is required to find luminosity.

With N_Λ and l calculated from the simulation, equation 4.2 gives us the luminosity of the Λ beam.

4.3 Acceptance

To properly do our analysis we must consider the detector efficiency. This efficiency is described using the acceptance. The acceptance is a measure of the efficiency of CLAS to detect the events of our experiment, $\Lambda p \rightarrow pp'\pi^-$. For example, the CLAS detector has six separate sectors, each of which has a gap between them. Obviously, in this space there should be no particles detected. However, that does not mean that there are no particles that get scattered into those regions. It simply means that the detector can not measure those regions well, or not at all. For particles in these blind areas the acceptance will be

zero, no particles get detected. If there was a region of the detector that was able to detect every event from our reaction, that region would have an acceptance of one. The acceptance is simply the ratio of the number of particles that get detected by the detector and the number that pass through. The efficiency will also depend on the kinematics of the reaction. For example, if we imagine that the detector does not do well at detecting particles at small angles, relative to the beam axis, then reactions which have high forward scattering will be less common to observe than reactions which have wide angular distributions. There is no physical reason for these forward scattering events to be less common, it is purely a feature of the detector. It is important to note that the detector efficiency is not necessarily low for small angles, but this example illustrates the importance of utilizing acceptance in calculation. In practice, a simulation is used to calculate the acceptance. The simulation must model both all events (generated events), and the detected events (accepted events).

4.3.1 Generated Events

First, events must be made in the simulation to represent all the particles that might be produced in the our reaction. This includes photons, protons, Λ and kaons. These particles were generated uniformly throughout the target with a uniform distribution of photon energy in the same range we observe in our data. These events shower the entire detector in all space and are taken as input for the software which is used to generate accepted events. Figure 4.3 shows the phase space distribution of the generated recoiled proton. This distribution is based purely on the kinematics of the particles. At this stage, there is still no detector information, only data from the simulated events.

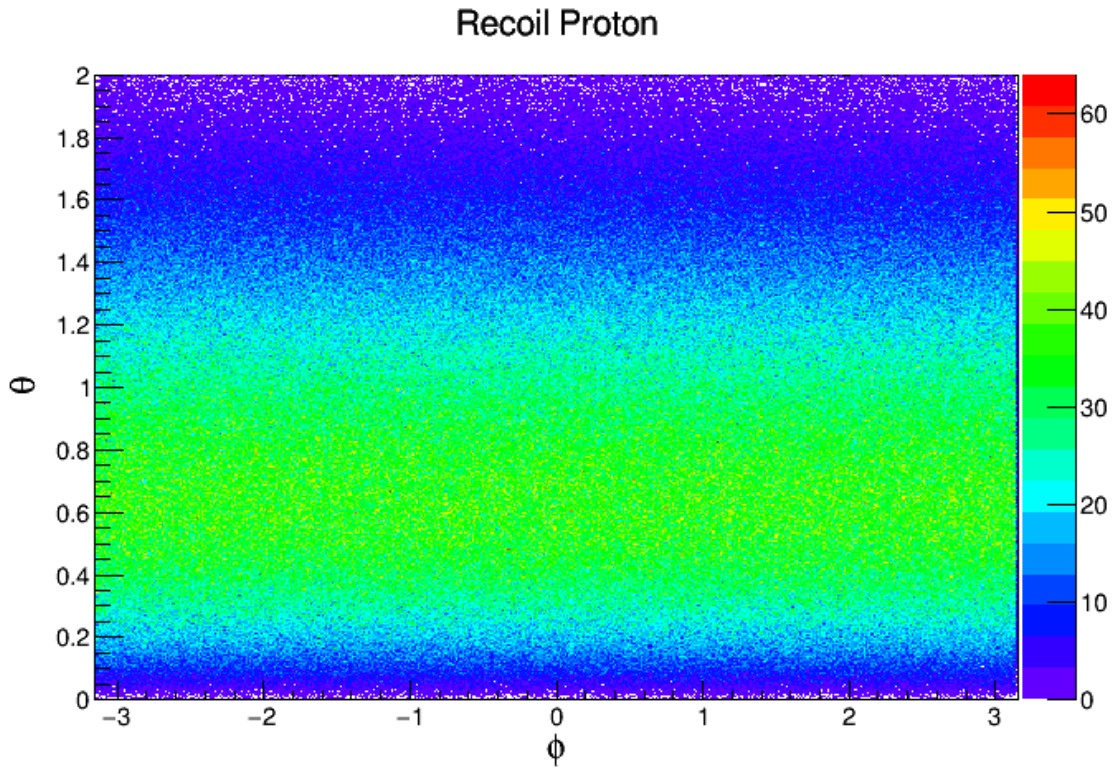

Figure 4.3: Phase Space of the generated recoil proton (in radians).

4.3.2 Accepted Events

The software used to get the accepted events is known as Geant [13]. This is a common software package used for simulations at various accelerator facilities. For use in this experiment, the software was set up to recreate the CLAS detector. By giving as input the four-vectors of each generated event, it should return a data stream that models real data. Figure 4.4a shows the same distribution as Figure 4.3, but only for accepted events. We can see that there regions of considerably more counts, and regions of no counts at all. This is because Geant recognizes that there are blind spots between the panels of the detector. Furthermore, the software also identifies other bad spots in the detector such as bad TOF paddles. It is also evident that the number of total counts is significantly lower

for the accepted events compared the the generated events. This makes sense because at best a perfect detector will yield the same number of accepted events as generated. By binning the accepted events and generated events with the same binning scheme as the data, we get an acceptance value for each yield, as discussed in section 4.1.

Figure 4.4 shows how the Monte Carlo compares to the data. We can see that both distributions are consistent which means the simulation can be trusted.

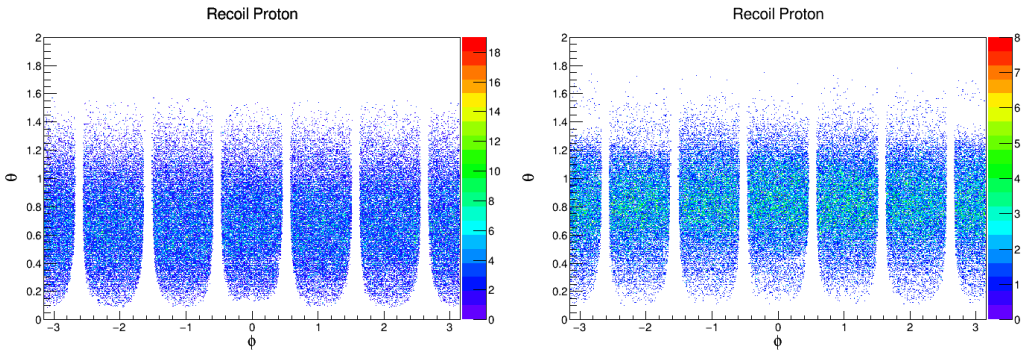

(a) Monte Carlo (b) Data

Figure 4.4: Phase Space of the recoiled proton for both the Monte Carlo simulation and the data (in radians).

We can see that the simulation matches well with the data, however we still need to extract the acceptance values. Since the data are binned in photon energy and Λ momentum, the same is done for the generated and accepted events. By counting the number of events in each bin and dividing the accepted events by the generated events, the acceptance for each bin can be extracted. Figure 4.5 shows the Monte Carlo and Figure 4.6 shows the generated data binned appropriately. All cuts which were made on the data is also made on the simulated data.

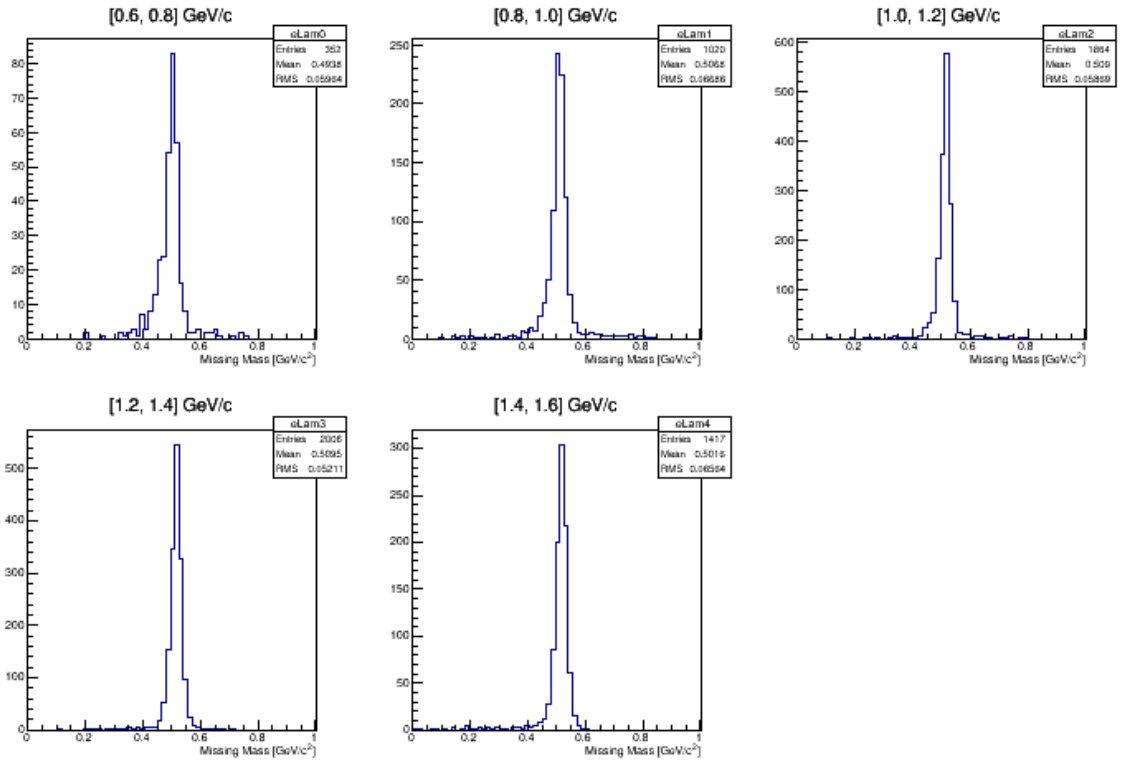

Figure 4.5: Accepted events binned in P_Λ in the same binning scheme as the data in Figure 4.1. The peak is for the simulated K^+ with no background and spread with the detector resolution.

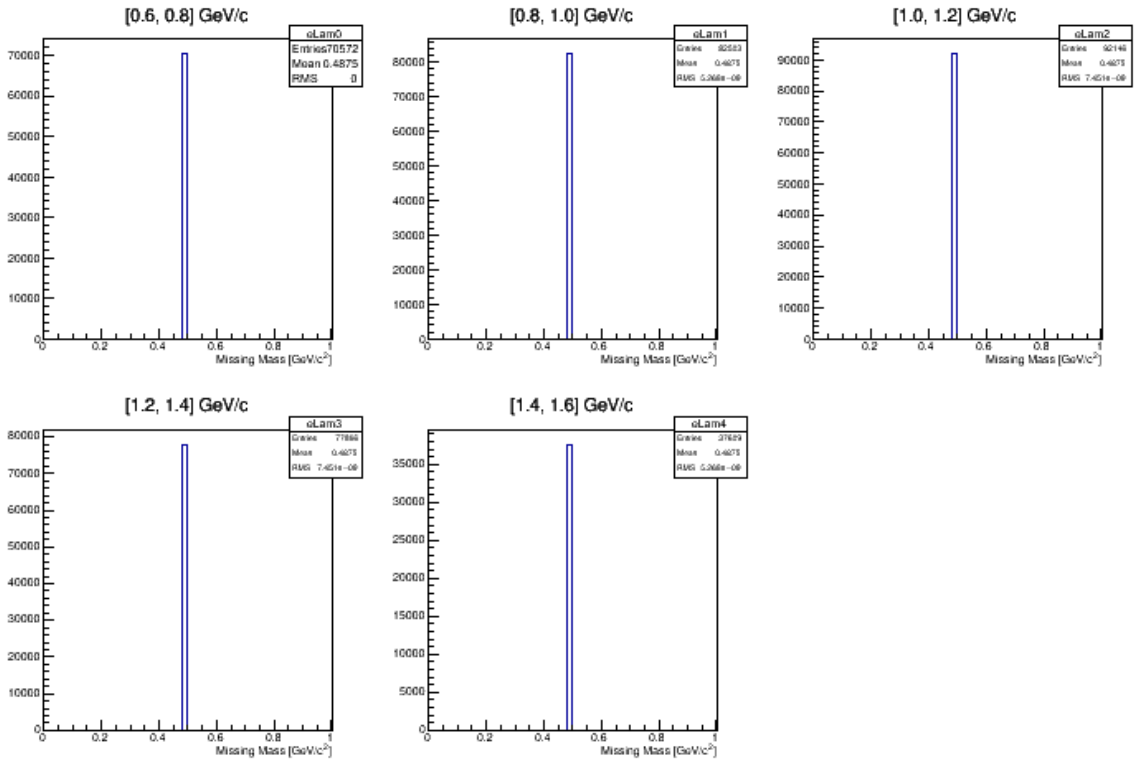

Figure 4.6: Generated events binned in P_Λ in the same binning scheme as the data in Figure 4.1. The spike is for the generated K^+ with no background and with no spreading due to detector resolution.

By fitting the Monte Carlo histograms to a Gaussian centered at the mass of the K^+, badly measured events can be removed. Integrating this Gaussian yields the number of accepted events for that momentum bin. For the case of the generated events, no fit is needed and the number of events in the histogram is the number of generated events. Figure 4.7 shows the acceptance for each bin, where each point is at the center of the Λ momentum range for the bin. For example, the bin where $0.8 GeV/c < P_\Lambda < 1.0 GeV/c$ the plot shows a point at $0.9 GeV/c$.

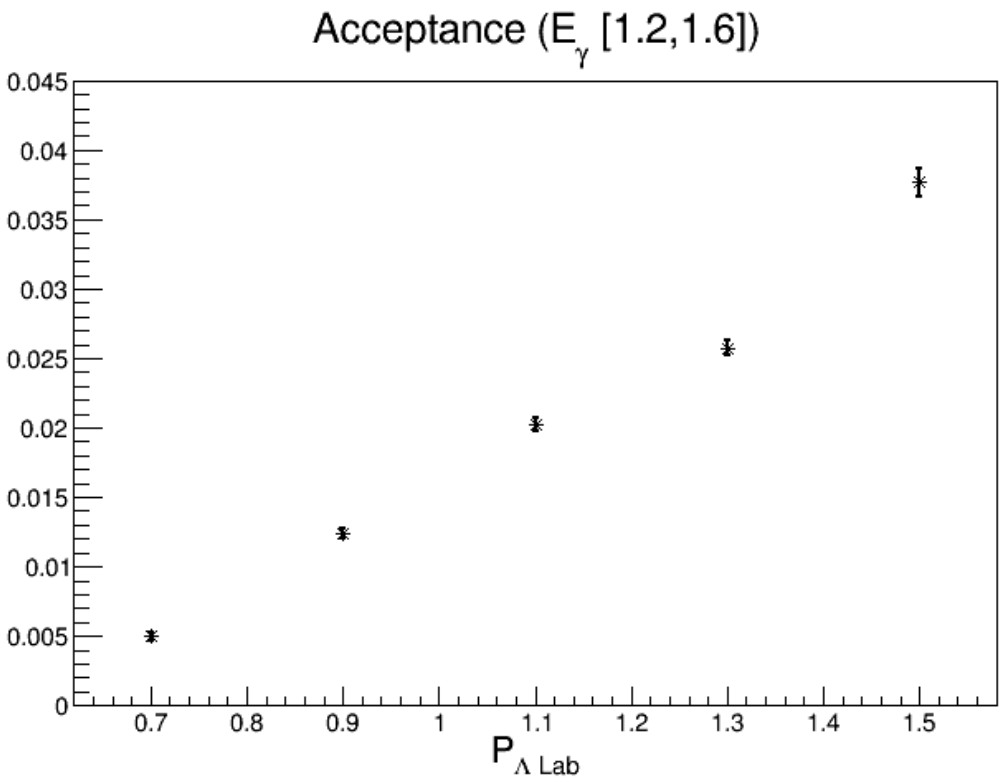

Figure 4.7: Acceptance binned in E_γ (units of GeV) and P_Λ (units of GeV/c).

The acceptance ranges between 0.5% and 4.5% and the error bars are purely from the statistical uncertainty.

5 Results and Future Work

With the yield, acceptance of the detector, and luminosity of the Λ beam, it is possible to calculate a cross-section for the Λ-N interaction. Figure 5.1 shows the total cross section, in millibarns (10^{-27} cm^2), with respect to the momentum of the incident Λ beam.

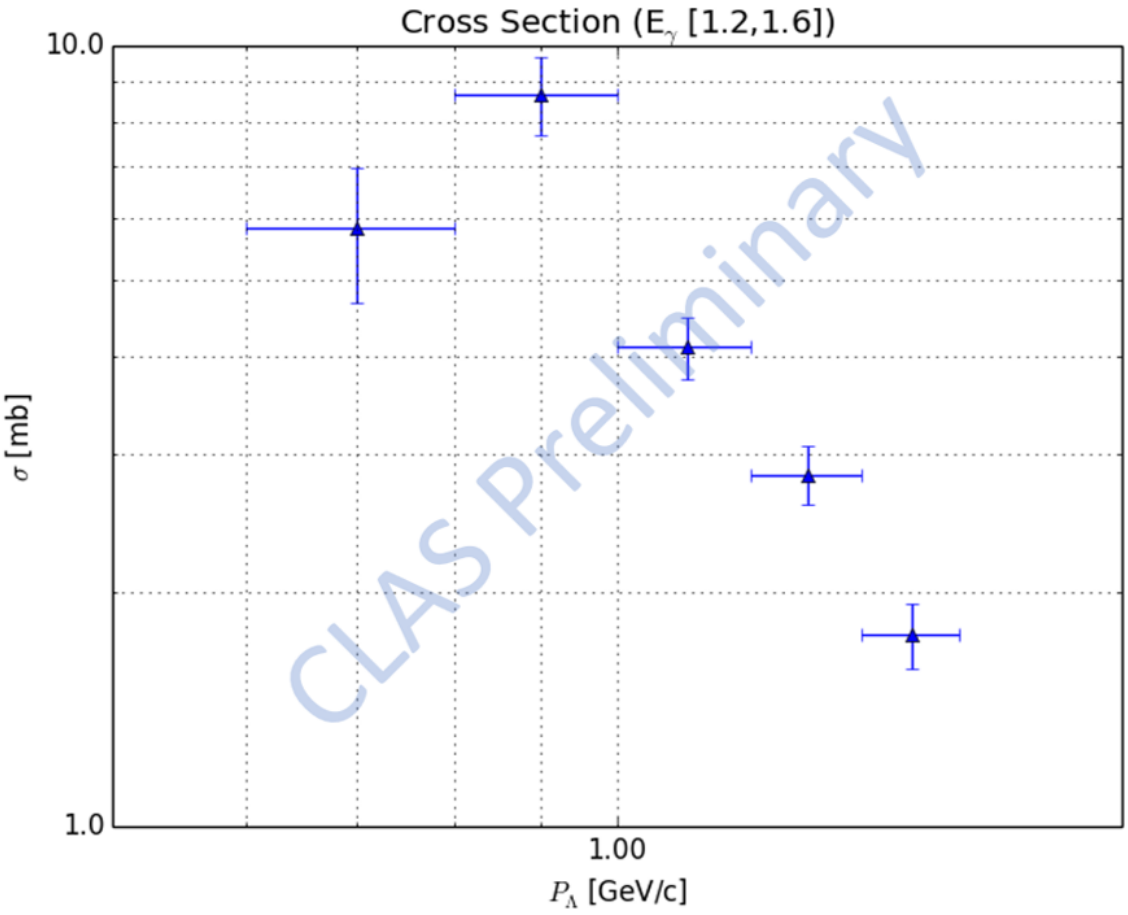

Figure 5.1: Cross section of the Λ-N elastic scattering interaction. Results are only for photon energy in the range 1.2-1.6 GeV. Error bars only represent statistical uncertainty.

The horizontal error bars comes from the size of the momentum bins where the yields were extracted. Comparing this data to that of existing data, this analysis yields results on the lower end of the existing data, as shown in Figure 5.2.

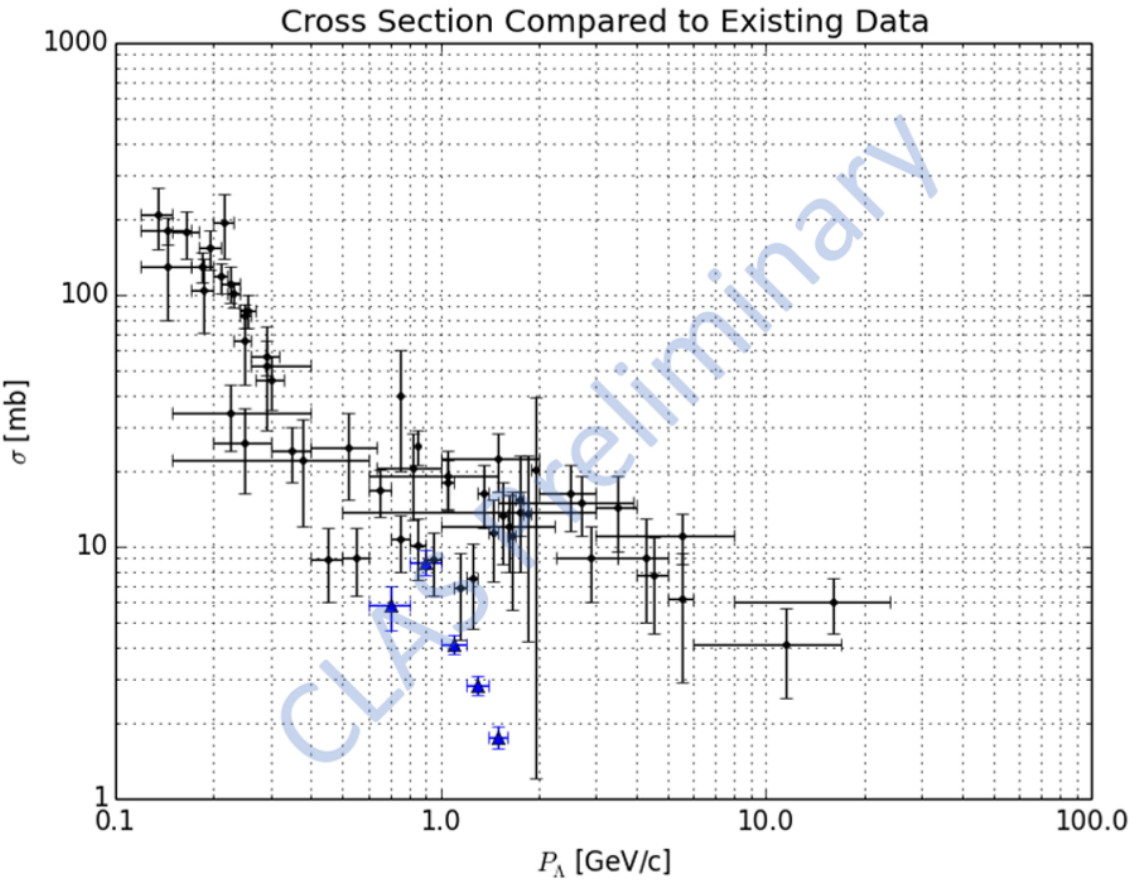

Figure 5.2: Comparing the cross section of the Λ-N elastic scattering interaction to existing data. Existing data is shown in black while results from this analysis are in blue.

For higher momentum, the cross-section drops below what is consistent with the existing data. However, the general shape of the cross section seems to agree with previous analysis. In the existing data there is a dip in the cross-section at a momentum of 0.5

GeV/c, followed by a peak and then a continuous decrease. This analysis shows a cross-section which behaves the same way.

The existing data has a larger momentum range than this analysis is able to observe. This is in part because Figure 1.1 is a collection of results from different experiments. What can be observed however is improved on. Currently the uncertainty is only from statistics, but even with systematic uncertainty taken into account (which is beyond the scope of this Masters thesis), the results should have smaller uncertainty than the current data. It is possible to also push the momentum range further and get cross sections at higher Λ momentum's. The results are only for events with incident photons in the range 1.2 to 1.6 GeV. There is data available from this experiment to extract yields from events with higher energies. There is additional data at higher photon energies, which would be a future direction for this research. It is not possible to get any lower in Λ momentum as the minimum photon energy in the experiment is 1.2 GeV which yields a minimum Λ momentum of around 0.6 GeV/c for our experimental setup.

REFERENCES

[1] D. Groom *et al.*, The European Physical Journal **C15**, 1+ (2000).

[2] J. Goetz, Ξ *Hyperon Photoproduction from Threshold to 5.4 GeV with the CEBAF Large Acceptance Spectrometer*, Ph.D. thesis, University of California, Los Angeles (2010).

[3] M. E. McCracken *et al.* (CLAS Collaboration), Phys. Rev. C **81**, 025201 (2010).

[4] B. Sechi-Zorn, B. Kehoe, J. Twitty, and R. A. Burnstein, Phys. Rev. **175**, 1735 (1968).

[5] S. S. Wong, *Introductory Nuclear Physics* (Prentice-Hall, Englewood Cliffs, New Jersey, 1990).

[6] B. A. Mecking *et al.* (CLAS), Nucl. Instrum. Meth. **A503**, 513 (2003).

[7] D. Sober *et al.*, Nuclear Instruments and Methods in Physics Research Section A: Accelerators, Spectrometers, Detectors and Associated Equipment **440**, 263 (2000).

[8] Y. Sharabian *et al.*, Nuclear Instruments and Methods in Physics Research Section A: Accelerators, Spectrometers, Detectors and Associated Equipment **556**, 246 (2006).

[9] M. Mestayer *et al.*, Nuclear Instruments and Methods in Physics Research Section A: Accelerators, Spectrometers, Detectors and Associated Equipment **449**, 81 (2000).

[10] E. Smith *et al.*, Nuclear Instruments and Methods in Physics Research Section A: Accelerators, Spectrometers, Detectors and Associated Equipment **432**, 265 (1999).

[11] C. Patrignani *et al.* (Particle Data Group), Chin. Phys. **C40**, 100001 (2016).

[12] S. Mandelstam, Phys. Rev. **112**, 1344 (1958).

[13] S. Agostinelli *et al.* (GEANT4), Nucl. Instrum. Meth. **A506**, 250 (2003).

Appendix A: Angular Dependence of Λ Beam

When a Λ is created in the target, it is created at some angle with respect to the photon beam axis. As discussed in Section 4.2 the angular distribution changes the path-length of Λ drastically. To calculate the angular distribution, we start at with the Lorentz invariant Mandlestam variable [11],

$$\begin{aligned} t &= (\boldsymbol{p_\gamma} - \boldsymbol{p_{K^+}})^2 = (\boldsymbol{p_p} - \boldsymbol{p_\Lambda})^2 \\ &= m_\gamma^2 - 2E_\gamma E_{K^+} + 2\vec{p_\gamma} \cdot \vec{p_{K^+}} + m_{K^+}^2 \qquad \text{(A.1)} \\ &= m_p^2 - 2E_p E_\Lambda + 2\vec{p_p} \cdot \vec{p_\Lambda} + m_\Lambda^2 \qquad \text{(A.2)} \end{aligned}$$

From A.1, the momentum of the photon is just its energy, which is known in the experiment from the tagger. Since the photon energy is entirely along the z-axis (defined by the beam line), we can rewrite A.1 as:

$$\begin{aligned} t &= m_\gamma^2 - 2E_\gamma E_{K^+} + 2\vec{p_\gamma} \cdot \vec{p_{K^+}} + m_{K^+}^2 \\ t &= m_\gamma^2 - 2E_\gamma E_{K^+} + 2|E_\gamma||p_{K^+}|cos(\theta) + m_{K^+}^2 \\ cos(\theta)_{K^+} &= \frac{t + 2E_\gamma E_{K^+} - m_{K^+}^2}{2E_\gamma p_{K^+}} \qquad \text{(A.3)} \end{aligned}$$

where θ is the angle of the scattered kaon (in the lab frame) with repect to the z-axis. We now need to find the unknowns: t, E_{K^+} and p_{K^+}.

From A.2, the mass of a photon is zero, and since the proton is at rest the energy is just its rest mass. So the equation becomes:

$$t = m_p^2 - 2m_p E_\Lambda + m_\Lambda^2 \qquad \text{(A.4)}$$

E_Λ is known if the momentum is known from $E_\Lambda = \sqrt{p_\Lambda^2 + m_\Lambda^2}$. The momentum is taken as a parameter to the simulation discussed in 4.2, so E_γ is a known quantity. E_K^+ can be

calculated using conservation of energy:

$$E_{initialstate} = E_{finalstate}$$
$$E_\gamma + E_p = E_{K^+} + E_\Lambda$$
$$E_{K^+} = E_\gamma + m_p - E_\Lambda \tag{A.5}$$

where E_p was replaced by m_p for a proton at rest. Since $p_{K^+} = \sqrt{E_{K^+}^2 - m_{K^+}^2}$, equation A.3 can be calculated.

A.1 Boosting from CM frame to Lab frame

The angular dependence taken from [3] is referring to the center of mass (CM) frame of the scattered kaon. In the CM frame, the angle of the scattered Λ will simply be 180^o - $\theta_{K^+}^{CM}$, which means the CM angle of Λ is known. Since this experiment occurs in the lab frame, a change of frame is required. The CM frame is only moving along the beam line compared to the lab frame. This means only the z-axis will be boosted while the x and y-axes remain unchanged. We can equate p_Λ^{CM} and p_Λ^{LAB} in the y-axis by,

$$p_{CM}\sin(\theta_{CM}) = p_{LAB}\sin(\theta_{LAB}) \tag{A.6}$$

where p_{CM} is the momentum of the Λ in the CM frame, and p_{LAB} is the momentum of Λ in the lab frame. This yields an angular dependence for the Λ in the lab frame:

$$\theta_{LAB} = \arcsin(\frac{p_{CM}}{p_{LAB}}\sin(\theta_{CM})) \tag{A.7}$$

which is required to simulate a physical Λ beam and calculate the luminosity.

Appendix B: Cross Section Sample Calculation

In this section we will go through a sample calculation to get the cross section value in momentum range 0.8 to 1.0 GeV/c shown in Figure 5.1. Once the final particles are properly identified as described in Chapter 3, the yield must be calculated. To do this, the missing mass distribution is binned in incident Λ momentum, p_Λ. These distributions are shown in 4.1. To extract the yield from the first bin, the background is fitted with an exponential function and the peak is fitted with a Gaussian function. The background is then removed and an integral is taken over the remaining Gaussian. The yield for this bin is 117 counts.

To calculate the acceptance, the missing mass distribution of generated events and accepted events must be binned in the same scheme as the data was when the yields were extracted. This binning is shown in Figure 4.5 and Figure 4.6. The number of events for the generated data in the momentum bin 0.8 to 1.0 GeV/c is 82503. The counts for the accepted data in the same bin is 972. Dividing these numbers, the acceptance for this momentum bin is 0.0118, or 1.118%.

Finally, the luminosity must be calculated. As explained in Section 4.2, there are two values which are needed to obtain a luminosity: the path length of the Λ and the number of Λ in the beam. Since the average path length is calculated from equation 4.3 which depends on the individual momentum of each particle, multiple particles will need to be created in the momentum range 0.8 to 1.0 GeV/c. From Appendix A we can calculate the angular dependence for Λ in this momentum range, and with the angular dependence and the path length the luminosity can be calculated. The average path length is calculated to be 3.08 cm. Since the luminosity of the photon beam can be measured, the number of Λ in the beam can be calculated from equation 4.4. The $K^+\Lambda$ cross section from Ref. 4.2 can be integrated within the angular range allowed by the momentum limits of the bin with results shown in Table B.1.

Table B.1: Results of a simulation of the Λ beam in the target with various inputs to calculate the number of Λ in the beam.

E_γ	$\sqrt{s}$	p_{low}	p_{high}	$\cos(\theta)_{low}$	$\cos(\theta)_{high}$	N_Λ
1.2	1.775	0.8	1.0	0.177	0.346	1.09×10^7
1.6	1.975	0.8	1.0	0.214	0.504	1.47×10^7

This yields an average Λ beam flux of 1.35×10^7 partilcles. From the known density of the target, $.071 \frac{g}{cm^3}$, the luminosity is:

$$L_\Lambda = N_\Lambda \times l \times \frac{.071 \frac{g}{cm^3} \times 6.02 \times 10^{23} \frac{1}{mol}}{1.0 \frac{g}{mol}} = 1.79 \times 10^{30} cm^{-2} \tag{B.1}$$

With the yield, acceptance and luminosity calculated, the cross section can be found:

$$\begin{aligned} \sigma &= \frac{Yield}{Acceptance \times Luminosity \times BranchingRatio} \\ \sigma &= \frac{117}{0.0118 \times 1.79 \times 10^{30} cm^{-2} \times .639} \\ \sigma &= 8.65\ mb \end{aligned} \tag{B.2}$$

Appendix C: Copyright/License Permissions

1. RNP/18/OCT/008761

Thesis and Dissertation Services